UNIVERSIDAD DE INVESTIGACIÓN DE TECNOLOGÍA EXPERIMENTAL YACHAY

Escuela de Ciencias Biológicas e Ingeniería

Determination of Radon Gas (^{222}Rn) Concentrations in Houses of San Miguel de Urcuquí

Trabajo de integración curricular presentado como requisito para la obtención del título de Ingeniero Biomédico

Autor:

Gutiérrez Guimi Jorge Andrés

Tutor:

Ph.D Ramírez Cando Lenin Javier

Urcuquí, junio del 2024

Autoría

Yo, **GUTIÉRREZ GUIMI JORGE ANDRÉS**, con cédula de identidad 1206017566, declaro que las ideas, juicios, valoraciones, interpretaciones, consultas bibliográficas, definiciones y conceptualizaciones expuestas en el presente trabajo; así cómo, los procedimientos y herramientas utilizadas en la investigación, son de absoluta responsabilidad de el autor del trabajo de integración curricular. Así mismo, me acojo a los reglamentos internos de la Universidad de Investigación de Tecnología Experimental Yachay.

Urcuquí, junio del 2024.

Jorge Andrés Gutiérrez Guimi

CI: 1206017566

Autorización de publicación

Yo, **GUTIÉRREZ GUIMI JORGE ANDRÉS**, con cédula de identidad 1206017566, cedo a la Universidad de Investigación de Tecnología Experimental Yachay, los derechos de publicación de la presente obra, sin que deba haber un reconocimiento económico por este concepto. Declaro además que el texto del presente trabajo de titulación no podrá ser cedido a ninguna empresa editorial para su publicación u otros fines, sin contar previamente con la autorización escrita de la Universidad.

Asimismo, autorizo a la Universidad que realice la digitalización y publicación de este trabajo de integración curricular en el repositorio virtual, de conformidad a lo dispuesto en el Art. 144 de la Ley Orgánica de Educación

Urcuquí, junio del 2024.

Jorge Andrés Gutiérrez Guimi

CI: 1206017566

Dedication

To God, my Lord, for His guidance and blessings.

To my beloved family, who have been a fundamental pillar in my education.

To my friends, for their unwavering support and companionship.

Jorge Andrés Gutiérrez Guimi

Acknowledgment

I extend my heartfelt gratitude to Professor Lenin Ramírez for his unwavering support and guidance throughout the realization of this project.

Special thanks to Professor Caterine Carrasco for generously lending me a radon detector, which proved instrumental in my research.

I am deeply thankful to all my friends and colleagues who assisted me in housing the sensors, their invaluable help made this project possible.

I am indebted to the dedicated faculty members of Yachay Tech whose mentorship and teachings have shaped me into a better scientist.

<div align="right">Jorge Andrés Gutiérrez Guimi</div>

Resumen

La exposición al radón en interiores es una causa significativa de cáncer de pulmón, solo superada por el tabaquismo [1]. La concentración de radón puede variar dependiendo de factores como la geología local, los materiales de construcción, la temperatura y la humedad relativa [1, 2]. Esta variación subraya la necesidad de realizar mediciones locales de radón para evaluar con los riesgos de exposición e implementar estrategias de mitigación.

En este estudio, se registraron mediciones de radón, temperatura y humedad utilizando tres detectores digitales de radón Corentium Home y tres dispositivos termómetros e higrómetros HTC-1. Los valores promedio diarios de radón a corto plazo se registraron tres veces al día durante una semana, junto con datos de temperatura y humedad. También se registró el promedio de medición a 7 días.

Treinta y seis casas ubicadas en la universidad Yachay Tech, Urcuquí, fueron estudiadas. Las casas fueron divididas en dos grupos: casas patrimoniales que cuentan con una infraestructura antigua y apartamentos multifamiliares de nueva construcción, fueron estudiadas durante siete días.

Los resultados mostraron correlaciones negativas entre el radón y la temperatura interior (tau = -0.30) y la diferencia de temperatura interior-exterior (tau = -0.21), y una correlación positiva con la humedad relativa (tau = 0.33). Las casas patrimoniales presentaron niveles de radón más altos que los apartamentos multifamiliares (test de Mann-Whitney, p = 5.14×10^{-7}). Las concentraciones promedio de radón encontradas estaban entre 2.96 y 130.98 Bq m^{-3}, con un promedio combinado de 20.58 Bq m^{-3} y una mediana de 13.88 Bq m^{-3}. Solo una casa superó el nivel de referencia de 100 Bq m^{-3} de la Organización Mundial de la Salud, por lo cual se recomienda realizar mediciones a largo en esta casa [1].

Palabras Clave:

Radón, Yachay Tech, humedad relativa, temperatura, HTC-1.

Abstract

Indoor radon exposure is a significant cause of lung cancer, second only to smoking [1]. Radon concentration can vary depending on factors such as local geology, building materials, temperature, and relative humidity [1, 2]. This variation underscores the need for localized radon measurements to assess exposure risks and implement mitigation strategies.

In this study, radon, temperature, and humidity measurements were recorded using three Corentium Home digital radon detectors and three HTC-1 temperature and hygrometer devices. Short-term daily average radon values were recorded three times a day over a week, alongside temperature and humidity data. The short-term 7-day average was also recorded.

Thirty-six houses located in Yachay Tech University, Urcuquí, were studied. The houses were divided into two groups, old-restored Patrimonial houses and newly built Multifamiliares apartments, were studied over seven days.

Results showed negative correlations between radon and indoor temperature (tau = -0.30) and indoor-outdoor temperature difference (tau = -0.21), and a positive correlation with relative humidity (tau = 0.33). Patrimonial houses exhibited higher levels of radon than Multifamiliares apartments (Mann-Whitney test, p-value = 5.14×10^{-7}). Average radon concentrations were found to be in the range of 2.96 to 130.95 Bq m^{-3} with a combined average of 20.58 Bq m^{-3} and a median of 13.88 Bq m^{-3}. Only one house exceeded the World Health Organization reference level of 100 Bq m^{-3}, therefore it is recommended to perform long-term measurements in this house [1].

Keywords:

Radon, Yachay Tech, relative humidity, temperature, HTC-1.

Contents

List of Abbreviations

A	Mass number
ALARA	As Low As Reasonably Achievable
BEIR VI	Committee on the Biological Effects of Ionizing Radiation
Bq	Becquerel
Bq m^{-3}	Becquerel per cubic meter
CAT	Catalase
CI	Confidence Interval
CR-39/PADC	Polyallyl Diglycol Carbonate
CRMs	Continuous radon monitors
D	Dose conversion factor
DNA	Deoxyribonucleic acid
E	Annual mean effective dose
EPA	Environmental Protection Agency
eV	electron-volt
F	Equilibrium factor
GSH-Px	Glutathione Peroxidase
Gy	Grays
H	Occupancy factor
ICRP	International Commission on Radiological Protection
LR-115	Cellulose nitrate film
MLDSs	Multiply Locally Damaged Sites
miRNA	micro-RNA
PHz	Peta hertz
POD	Peroxidase

RH	Relative Humidity
ROS	Reactive Oxygen Species
SI	International System of Units
Sv	Sieverts
T	Number of hours in a year
WL	Working Levels
WLM	Working Level Months
WHO	World Health Organization
Z	Atomic number
^{14}**C**	carbon-14
^{206}**Pb**	lead-206
^{218}**Po**	Polonium-218
^{214}**Po**	Polonium-214
^{219}**Rn**	radon-219
^{220}**Rn**	radon-220
^{222}**Rn**	radon-222
^{226}**Ra**	radium-226
^{230}**Th**	thoron-230
^{234}**U**	uranium-234
^{238}**U**	uranium-238

List of Tables

List of Figures

List of Equations

Chapter 1

Introduction

1.1   Thesis Overview

Chapter 1 presents the introduction to this project, providing the background related to radon and its relationship with lung cancer. It highlights the importance of addressing indoor measurements, and outlines the problems and objectives of this investigation.

Chapter 2 covers the theoretical framework necessary to understand this study. It explains what radiation is, the different types of radiation, how radiation affects human bodies, radioactive decays, radiation dose, and the phenomena that explain radon movement such as convection, diffusion, and stack effect.

Chapter 3 delves into all theory related to radon. It explains the link between radon and increased risk of lung cancer, the origin of radon, its transportation into buildings, and the exposure pathways through which radon affects us. It also details Radon-induced carcinogenesis mechanisms, methods to detect radon, types of detectors, radon reference levels and regulations, similar works measuring indoor radon concentrations in houses, and radon studies performed in Ecuador.

Chapter 4 describes the methodology used in this study, including the criteria for selecting the studied houses, the sensors used and their operation, the protocol for sensor placement and data recording, and the formulas applied in the analysis.

Chapter 5 presents the results and discussion of the findings. It uses bar plots and box plots to aid in the interpretation and comparison of data between houses. An indoor radon

map is created with short-term 7-day average radon concentration. Statistical analyses are conducted to examine correlations between temperature and relative humidity with radon, and to compare radon concentrations between Patrimonial houses and Multifamiliares apartments. The limitations of this study are also discussed, and the results are compared with those in the literature.

Chapter 6 provides the conclusions of this study, including a summary of the study, the findings, and their comparison with the literature. Additionally, it offers recommendations for future research to authors interested in conducting similar studies.

1.2 Background

Radon is a naturally occurring radioactive gas that may be found in high concentrations in indoor environments such as homes, schools, and at the workplace [17]. The primary sources of residential radon are soils and rocks around the foundation, fuels, building materials, and domestic water [17]. Indoor radon concentration can vary greatly from 10 $\mathrm{Bq\,m^{-3}}$ to more than 10,000 $\mathrm{Bq\,m^{-3}}$ [17]. According to the World Health Organization (WHO), radon is a significant health risk, and for most people, the greatest exposure to radon occurs in the home where people spend much of their time [1].

An increased rate of lung cancer was first seen in uranium miners exposed to very high concentrations of radon. In addition, studies in Europe, North America, and China have confirmed that even low concentrations of radon – such as those commonly found in residential settings – also pose health risks and contribute to the occurrence of lung cancers worldwide [1].

Radon gas is an important source of ionizing radiation of natural origin and a major contributor to the ionizing radiation dose received by the general population [18]. Radon formed by the decay of radium in soil and rocks and entering the indoor air spaces of buildings or other enclosed locations (such as mines, tunnels, or other underground work-places) may reach concentrations of concern for health [18]. Most of the radiation dose and hence the risk from radon is due to its short-lived alpha-particle-emitting polonium decay products (^{218}Po and ^{214}Po) [18].

To reduce the risk of radon exposure, it is recommended to measure residential radon

levels in an inexpensive and simple manner by means of small passive detectors [17]. The WHO recommends that the reference level for radon in homes should be 100 $Bq\,m^{-3}$ or lower [17]. The U.S. Environmental Protection Agency (EPA) recommends installing a radon reduction system if the radon level is at or above 148 $Bq\,m^{-3}$ of air [1]. It is also recommended to test for radon levels before and after any renovations, especially after making any repairs to reduce radon levels [1].

1.3 Problem Statement

Indoor radon exposure is a major cause of lung cancer worldwide, recognized as the second leading cause of lung cancer after smoking and the primary cause for non-smokers [1]. Radon is an odorless, tasteless, and invisible noble gas that originates from the decay of uranium-238 (^{238}U) found ubiquitously in the earth's crust [2]. Through a series of decay processes, 238U produces radium-226 (^{226}Ra), which further decays to radon-222 (^{222}Rn) [2], an isotope with a significant half-life that allows it to accumulate in indoor environments [2].

The concentration of radon in buildings is influenced by various factors such as local geology, building materials, construction methods, and environmental conditions like temperature and humidity [2]. Radon can infiltrate homes through cracks in foundations and other openings, resulting in varying levels of indoor radon even between adjacent buildings [2]. Studies have consistently shown a strong relationship between indoor radon levels and lung cancer risk, with an estimated increase in lung cancer risk of 8% to 13% per 100 $Bq\,m^{-3}$ increase in radon exposure [1].

In Ecuador, indoor radon levels have been found to be among the highest in South America, with concentrations ranging from 20.39 to 225.66 $Bq\,m^{-3}$ and an average of 94.30 $Bq\,m^{-3}$ in some studies [19]. These variations highlight the need for localized radon measurements to assess exposure risks accurately and implement mitigation strategies where necessary.

This thesis aims to address the problem of indoor radon exposure by measuring radon levels in San Miguel de Urcuquí, specifically in houses on the Yachay Tech campus. The study will compare radon concentrations in old-restored houses (Patrimonial houses) and

newly built houses (Multifamiliares apartments). Additionally, it will investigate the relationship between indoor radon levels and factors such as indoor relative humidity and temperature.

To achieve this, three Corentium Home digital radon detectors were used to perform short-term measurements over seven days in 36 houses. Data on indoor and outdoor temperature and relative humidity were also collected to explore correlations with radon levels. This research will contribute to the existing knowledge base by providing localized data on indoor radon levels and identifying factors influencing radon accumulation, thus aiding in the development of effective radon mitigation strategies.

The significance of this study lies in its potential to improve public health by reducing radon exposure and the associated risk of lung cancer, particularly in regions with high radon concentrations like Ecuador. By understanding the dynamics of radon levels in different types of houses and under various environmental conditions, this research can inform guidelines and policies for radon measurement and mitigation, ultimately contributing to safer indoor environments.

1.4   Objectives

1.4.1   General Objective

To evaluate indoor radon concentrations in housing units on the Yachay Tech University campus, with a focus on understanding the differences between old-restored houses and newly constructed houses.

1.4.2   Specific Objectives

(i) **Measure Radon Concentration:** Conduct short-term (7-day) measurements of ^{222}Rn concentrations in 36 houses on the Yachay Tech campus using Corentium Home digital radon detectors.

(ii) **Record Environmental Data:** Collect daily data on indoor and outdoor temperature, as well as indoor relative humidity, to examine their potential influence on radon levels.

(iii) **Compare House Types:** Analyze and compare radon concentrations between old-restored houses (Patrimonial houses) and newly built houses (Multifamiliares apartments).

(iv) **Create a Radon Map:** Develop an indoor radon concentration map for the Yachay Tech campus based on the short-term 7-day measurement data, highlighting areas with higher radon levels.

(v) **Calculate Effective Dose:** Estimate the annual effective dose of radon exposure for residents based on the measured radon concentrations.

(vi) **Identify Correlations:** Investigate the correlations between indoor radon levels and indoor environmental factors such as relative humidity and temperature differences.

Chapter 2

Theoretical Framework

2.1 Introduction to Radiation

Radiation can be understood as a form of energy transport from a source that travels in the form of particles or waves [20]. According to its capability to ionize an atom or molecule, radiation can be classified into non-ionizing and ionizing radiation [20].

2.2 Non-Ionizing Radiation

Non-ionizing radiation is a form of radiation that does not possess enough energy to trigger an ionization process, i.e., sufficient energy to expel electrons from their orbitals [21]. According to the International Commission on Non-Ionizing Radiation Protection (ICNIRP), non-ionizing radiation refers to electromagnetic radiations and fields with photon energy below 10 eV. This corresponds to frequencies below 3 PHz and wavelengths longer than 100 nm [22].

There are different sources of non-ionizing in daily life, for example, microwave ovens, computers, cell phones, and wireless monitors [23]. In the medical context, non-ionizing radiation is used in applications such as ultrasound imaging, laser surgery, and magnetic resonance imaging [24].

2.3   Ionizing Radiation

Ionization is the process by which an atom or molecule gains or loses electrons, resulting in the formation of ions [25]. This can occur through various means such as collisions with subatomic particles, other atoms, molecules, or through interactions with electromagnetic radiation [25]. Ionization can lead to the creation of positively or negatively charged ions, which play a crucial role in various scientific and medical applications, including radiation detectors, mass spectrometry, and radiation therapy [25].

Ionizing radiation is a form of radiation that consists of particles and photons with enough energy to ionize atoms in the human body, leading to chemical changes that can have biological implications for cells [26]. Humans have always been exposed to ionizing radiation from natural sources, such as extraterrestrial and terrestrial gamma radiation, radioactive elements [26]. Ionizing radiation can also be generated through nuclear reactions, high temperatures, or the acceleration of charged particles in electromagnetic fields [25]. Artificial sources include nuclear reactors, particle accelerators, and medical devices [25].

2.3.1   Interaction of Ionizing Radiation with Matter

When ionizing radiation interacts with biological matter, it can have various effects on cells and tissues [27]. The interaction can be direct, where the radiation interacts directly with the critical target in the cell, or indirect, where the radiation interacts with other molecules and atoms within the cell to produce free radicals [28]. The interaction mechanism depends on the type of ionizing radiation, such as heavy charged particles, electrons, positrons, protons, and photons [28]. Charged particles, such as electrons, positrons, protons, and alpha particles, will ionize matter in a direct way, in contrast to neutral particles [28].

Reactive oxygen species (ROS) and free radical attacks are closely related phenomena in biological systems [29]. Free radicals are highly reactive chemical species with unpaired electrons, while ROS are a subset of free radicals that contain oxygen [29]. Common ROS include the hydroxyl radical, superoxide anion, and hydrogen peroxide [29]. These molecules play crucial roles in various physiological processes but can also cause damage when their production exceeds the body's antioxidant defenses, leading to oxidative stress

[29]. When free radicals attack, they can initiate chain reactions that damage cell components like lipids, proteins, and nucleic acids, ultimately causing tissue injury [29]. The hydroxyl radical is particularly efficient in these attacks [29]. To counteract the harmful effects of free radicals and ROS, the body relies on antioxidants [29]. Enzymatic antioxidants like superoxide dismutase, Glutathion Peroxidase (GSH-Px), Peroxidise (POD), and Catalase (CAT) convert harmful ROS into less toxic substances like hydrogen peroxide and water [29]. Non-enzymatic antioxidants such as glutathione, Vitamin E, and Vitamin C directly react with radicals to neutralize them [29]. Figure 2.1 is an schematic representation of the process of active oxygen metabolism in cells by irradiation made by Jia et al [6].
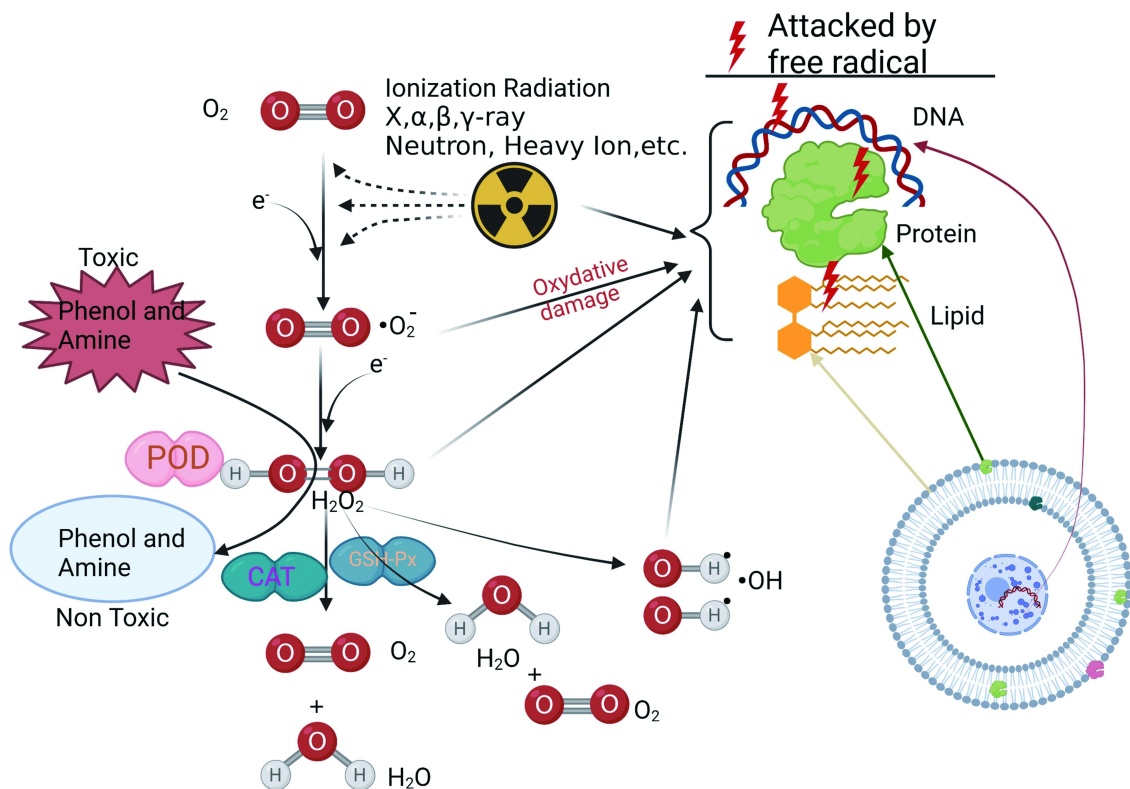
Figure 2.1: The process of active oxygen metabolism in cells by irradiation. Image created by Jia et al [6]. Used under the Creative Commons Attribution 4.0 International License (https://creativecommons.org/licenses/by/4.0/). No changes were made to the image.

Heavy charged particles, such as alpha particles, can cause significant ionization and excitation in matter due to their high mass and charge [27]. Electrons can also cause ionization and excitation, but their effect is less significant than that of heavy charged particles due to their lower mass [27]. Photons, such as X-rays and gamma rays, can interact

with matter through the photoelectric effect, Compton scattering, and pair production [27].

2.4 Radioactive Decay

Radioactive decay is a process in which unstable atomic nuclei lose energy by emitting radiation [30]. Through the process of radioactive decay, unstable isotopes transform into more stable elements by shedding one or more subatomic particles, which are known as radiation [30]. There are three common types of radioactive decay: alpha, beta, gamma decay [30].

2.4.1 Alpha Decay

Alpha decay is a type of radioactive decay in which an unstable atomic nucleus emits an alpha particle, which is composed of two protons and two neutrons [31, 32, 33]. The ejected particle is simply a helium nucleus, and it has a relatively large mass and a positive charge [31, 32, 33]. In equation 2.1, it can be seen the general equation representing alpha decay.

$$_Z^A X \rightarrow _{Z-2}^{A-4} Y + _2^4 \text{He} \tag{2.1}$$

Where X is the parent nucleus, Y is the daughter nucleus, A is the mass number, and Z is the atomic number.

Emitted alpha particles are slowed down by the attraction of nearby electrons until it captures two electrons and becomes a stable atom of helium [31, 32, 33]. Thus, alpha particles have a high ionizing power, but low penetrating power that even a sheet of paper can stop them [31, 32, 33].

2.4.2 Beta Decay

Beta decay is a type of radioactive decay in which a nucleus emits a beta particle, which can be either an electron or a positron, and a neutrino or an antineutrino [31, 32, 33]. Beta decay occurs when a nucleus has too many protons or too many neutrons, and one

of the protons or neutrons is transformed into the other [31, 32, 33]. Beta particles have low ionizing power, but higher penetrating power than alpha particles [31, 32, 33].

Beta minus decay

In beta minus decay, a neutron in a nucleus decays into a proton, emitting an electron and an antineutrino [31, 32, 33]. In equation 2.2, it can be seen the general equation for beta minus decay.

$$_Z^A X_N \rightarrow_{Z+1}^A X'_{N-1} + e^- + \bar{\nu}_e \tag{2.2}$$

Where X represents the parent nucleus, X' represents the daughter nucleus, A is the mass number, Z is the atomic number, $\bar{\nu}_e$ is the antineutrino, and N is the neutron number.

In this process, the mass number remains the same, but the atomic number increases by one while the neutron number decreases by one [31, 32, 33]. Beta minus decay occurs in neutron-rich nuclei and is a means for the nucleus to become more stable by converting a neutron into a proton [31, 32, 33].

Beta plus decay

Beta plus decay, also known as positron emission, is a type of radioactive decay in which a proton in the nucleus of an atom is converted into a neutron, releasing a positron and a neutrino [31, 32, 33]. In equation 2.3, it can be seen the general equation for beta plus decay.
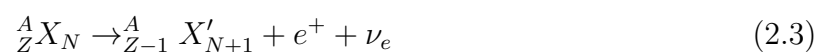
$$_Z^A X_N \rightarrow_{Z-1}^A X'_{N+1} + e^+ + \nu_e \tag{2.3}$$

Where X represents the parent nucleus, X' represents the daughter nucleus, A is the mass number, Z is the atomic number, ν_e is the neutrino, and N is the neutron number. In this process, the mass number remains the same, but the atomic number decreases by one while the neutron number increases by one [31, 32, 33]. Beta plus decay occurs in

proton-rich nuclei and is a means for the nucleus to become more stable by converting a proton into a neutron [31, 32, 33].

2.4.3   Gamma Decay

Gamma decay is a type of radioactive decay that occurs when a nucleus is in an excited state and releases energy in the form of a gamma ray photon [31, 32, 33]. Gamma decay usually occurs after other forms of decay, such as alpha or beta decay, have occurred [31, 32, 33]. When a radioactive nucleus undergoes alpha or beta decay, the daughter nucleus that results is usually left in an excited state [31, 32, 33]. The excited nucleus can then decay to a lower energy state by emitting a gamma ray photon [31, 32, 33].

2.5   Decay Chain

A decay chain, also known as a radioactive cascade, refers to a series of radioactive decays of different radioactive decay products as a sequential series of transformations [31, 32, 33]. When a radioactive atom undergoes decay, it emits energy in the form of ionizing radiation, such as alpha particles, beta particles, or gamma rays [31, 32, 33]. The decay products created during this process form a chain of subsequent decays until a stable isotope is reached [31, 32, 33].

Each decay chain is unique and specific to a particular radioactive isotope [31, 32, 33]. For example, the decay chain of ^{238}U culminates in lead-206 (^{206}Pb), with intermediate products such as uranium-234 (^{234}U), thoron-230 (^{230}Th), ^{226}Ra, and ^{222}Rn [31, 32, 33]. The decay products within the chain are always radioactive [31, 32, 33].

2.6   Nuclear Fission and Fusion

Nuclear fission and fusion are both nuclear processes, meaning they involve changes to the nucleus of atoms [34]. Nuclear fission is a process where a heavy nucleus breaks apart into lighter nuclei [34]. This process often results in the creation of very radioactive and unstable byproducts [34]. These byproducts continue to break down in a nuclear chain reaction, which can be seen as a form of radioactive decay [34].

On the other hand, nuclear fusion is a process where two light nuclei fuse together to form a heavier nucleus [35]. Fusion does not create any long-lived radioactive nuclear waste [35]. However, it does release neutrons, which can make other materials radioactive [35].

2.7 Half-Life and Radioactive Activity

Half-life is the time it takes for half of the radioactive nuclei in a sample to undergo radioactive decay, transforming into different elements or isotopes through processes such as alpha decay or beta decay [31, 32, 33]. Every radioactive isotope has a specific half-life, which can range from fractions of a second to billions of years [31, 32, 33]. For example, the half-life of carbon-14 (^{14}C) is 5,700 years, which means that if you start with a sample of ^{14}C, after 5,700 years half of the ^{14}C will have decayed into ^{14}N [31, 32, 33].

Radioactive activity refers to the number of radioactive nuclei that decay per unit time, often expressed as disintegrations per second [31, 32, 33]. The International System of Units (SI) unit for activity is Becquerel (Bq). The activity of a radioactive substance depends on two things: the amount of the radioactive substance present, and its half-life [31, 32, 33]. The greater the number of radioactive nuclei present in the sample, the more will decay per unit of time [31, 32, 33]. The shorter the half-life, the more decays per unit time, for a given number of nuclei [31, 32, 33].

2.8 Radiation Dose

Exposure to radiation can be quantified using various measures of radiation dose [3]. The International Commission on Radiological Protection (ICRP) defines three primary types of dose for radiological protection: absorbed dose, equivalent dose, and effective dose [3]. These definitions and guidelines are outlined in ICRP Publication 103, which serves as a comprehensive reference for radiological protection standards and practices.

2.8.1 Absorbed Dose

Absorbed dose can be understood as the amount of energy deposited by radiation in a mass. It is the basic physical dose quantity, and its units are $J\,kg^{-1}$. Absorbed dose is also

expressed in Grays (Gy) [3].

2.8.2   Equivalent Dose

Equivalent dose is used to calculate doses on individual organs or tissue and includes a radiation weighting factor in its calculation [3]. Thus, the type of radiation plays an important role. ICRP recommended radiation weighting factors are presented in Table 2.1.

Table 2.1: ICRP Recommended radiation weighting factors [3].

Radiation Type	Radiation Weighting Factor
Photons	1
Electrons and muons	1
Protons and charged Pions	2
Alpha particles, fission fragments, heavy ions	20

Since the radiation weighting factor is dimensionless, the unit for equivalent dose is $J\,kg^{-1}$ and is expressed in Sieverts (Sv). When expressing equivalent dose value, it has to be accompanied with the name of the organ [3].

2.8.3   Effective Dose

Effective dose calculation is used when different tissues and organs are included in the study [3]. Each organ is adjusted by a tissue weighting factor to take into consideration the sensitivity of the organ to radiation [3]. Thus, effective dose is calculated as the tissue-weighted sum of equivalent doses [3]. In Table 2.2, the recommended tissue weighting factors by the ICRP are shown. The unit for equivalent dose is $J\,kg^{-1}$ and is expressed in sieverts [3].

2.9   Radon Transport Mechanisms

Radon diffusion and convection are two primary mechanisms by which radon gas migrates through various materials and environments [36, 37]. These processes are crucial in understanding the behavior of radon in different settings, such as in soil, buildings, and during

Table 2.2: ICRP recommended tissue weighting factors for radiation exposure [3].

Tissue	Tissue Weighting Factor
Bone-marrow (red), Colon, Lung, Stomach, Breast	0.12
Gonads	0.08
Bladder, Oesophagus, Liver, Thyroid	0.04
Bone surface, Brain, Salivary glands, Skin	0.01

experiments [36, 37].

2.9.1 Radon Diffusion

Radon diffusion occurs when radon atoms move from an area of higher concentration to an area of lower concentration through a porous medium, such as soil, coal, or building materials [36, 37]. This process is governed by Fick's law, which describes the movement of radon as a function of the concentration gradient and the diffusion coefficient of the medium [36, 37]. The diffusion coefficient is a measure of the ease with which radon can move through a material, and it varies depending on the material's porosity, radium concentration, and other factors [36, 37].

Brownian motion

Diffusion due to Brownian motion is a phenomenon where the random movements of particles, known as Brownian motion, lead to the spreading out of particles in a fluid. This process is a result of the continuous collisions of particles with each other in the fluid, causing them to move randomly and spread out [38].

2.9.2 Radon Convection

Convection, or advection for the case of radon, is the movement of radon gas due to differences in pressure and temperature [36, 37]. This process is driven by the density differences between radon-rich and radon-poor areas, which can occur due to temperature gradients or changes in air pressure [36, 37].

2.9.3   Convection and Diffusion

Both Diffusion and convection play important roles in understanding radon migration [36, 37]. Diffusion is the primary mechanism in many situations, such as in soil or through building materials, where the movement of radon is driven by concentration gradients [36, 37]. Convection, however, becomes significant when there are significant temperature or pressure gradients present, such as in areas with significant temperature differences or in situations where air pressure changes occur [36, 37].

2.9.4   Stack Effect

The stack effect, also known as the chimney effect, is a phenomenon driven by thermal differences that cause air movement in buildings [39]. It occurs due to variations in indoor and outdoor air density resulting from differences in temperature and moisture levels [39]. In simpler terms, warm air rises because it is less dense than cold air, creating a pressure difference that leads to air movement [39]. The intensity of the stack effect is influenced by factors such as building height, the permeability of the building's facade cladding, wind force and direction, and the type of ventilation system in place [39]. Essentially, the stack effect describes how air naturally flows through a building based on these thermal and pressure differentials [39].

Chapter 3

Radon

3.1   Introduction

Radon is a naturally occurring odorless, colorless, and tasteless radioactive noble gas [40]. Radon constitutes the most significant proportion of radiation exposure originating from natural sources [40]. Moreover, radon tends to accumulate in closed spaces such as buildings and dwellings. Thus, it is the most important contributor to annual radiation dose to the population [41, 42].

3.2   Radon Exposure and Lung Cancer Risk

The understanding of radon exposure and its association with lung cancer has evolved significantly over time, marked by several studies and pivotal reports [1]. The historical roots of this understanding trace back to the sixteenth century, where evidence of increased mortality from respiratory disease among certain groups of underground miners in central Europe emerged [1, 43]. However, it was not until the nineteenth century that this disease was recognized as lung cancer[1, 43].

3.2.1   Lung Cancer Risks in Radon-Exposed Miners

The study of lung cancer risks in radon-exposed miners has been pivotal in understanding the relationship between radon exposure and lung cancer incidence [1]. Initially, cohort

designs were employed, tracking miners over time to establish vital status and ascertain causes of death [1]. However, early studies faced challenges in exposure assessment due to the lack of radon measurements, particularly in the earlier years of mining when exposures were highest [1].

The concept of Working Levels (WL) was introduced to quantify radon progeny concentrations, with cumulative exposure measured in Working Level Months (WLM) [1]. Despite methodological variations across studies, a review by the Committee on the Biological Effects of Ionizing Radiation (BEIR VI) in the 1990s highlighted a consistent trend of increasing lung cancer rates with cumulative radon exposure, although with substantial variation in risk magnitudes between studies [44].

BEIR VI conducted pooled analyses, estimating an average increase in lung cancer death rate per WLM [44]. Interestingly, this risk varied with time since exposure and age at exposure, with younger ages showing higher percentage increases in risk [1, 44]. Additionally, miners exposed to lower radon concentrations exhibited larger percentage increases in lung cancer death rates per WLM compared to those exposed to higher concentrations [1, 44]. Subsequent studies and follow-ups, including those in Czechia, France, Poland, Brazil, and Germany, further elucidated these findings, providing additional insights into the long-term effects of radon exposure on lung cancer mortality [1].

3.2.2 Lung Cancer Risks in the General Population from Indoor Radon

There is certain ambiguity that rise from numerical extrapolations from the miner studies, however, this can be solved by directly investigating the relationship between indoor radon and lung cancer risk [1]. In such research, radon exposure is typically quantified as the average radon gas concentration per cubic meter of air that an individual has been exposed to in their home over several past decades [1]. The unit used is Becquerel per cubic meter ($Bq\,m^{-3}$), where 1 Bq is defined as one disintegration per second [1].

Assessing radon exposure in homes presents unique difficulties due to fluctuating concentrations influenced by factors like seasonal variations and occupant behavior [1]. Initial attempts at understanding this relationship involved geographical correlation studies, but

their limitations in controlling for confounding factors like smoking rendered them inadequate [1].

Subsequently, case-control studies emerged as a more suitable approach, enabling researchers to compare radon exposure histories between individuals with and without lung cancer while controlling for smoking and other relevant factors [1]. Despite over 40 case-control studies conducted, individual studies often lacked statistical power to provide definitive conclusions [1]. To address this, systematic reviews and pooled analyses have been performed, revealing significant variations in risk estimates across studies [1].

Efforts to standardize data collection and analysis methods have been made to facilitate meaningful comparisons between studies and derive pooled risk estimates [1]. Notably, analyses of European, North American, and Chinese studies have supported the derivation of pooled risk estimates, underscoring the importance of collaborative efforts in advancing our understanding of the association between indoor radon exposure and lung cancer risk [1].

The European pooling study

Darby et al. conducted a pooled analysis which included thirteen studies spanning various countries including Austria, the Czech Republic, Finland, France, Germany, Italy, Spain, Sweden, and the United Kingdom [45]. They analyzed data from 7,148 individuals with lung cancer and 14,208 controls, considering both smoking and radon exposure histories, the latter measured over a 30-year period. The mean residential radon concentration among those with lung cancer was found to be $104\ \mathrm{Bq\,m^{-3}}$.

Using linear models, the researchers observed a significant association (p = 0.0007) between residential radon exposure over 35 years and lung cancer risk, with a linear dose-response relationship. The estimated excess relative risk for a $100\ \mathrm{Bq\,m^{-3}}$ increase in radon concentration was 0.08 (95% CI 0.03–0.16). Notably, this relationship held consistent across various studies and was not influenced by individual study characteristics or demographic factors such as age, sex, or smoking status.

The North American pooling study

The North American Pooling study, conducted by Krewski et al., compiled data from 3,662 cases and 4,966 controls across seven studies in the USA and Canada, mirroring the methodology of the European study [46]. Similar to its European counterpart, once individual subject data were consolidated, the radon-related risks across the component studies remained consistent.

Pooling data from all seven studies revealed an 11% increase in lung cancer risk per 100 $\mathrm{Bq\,m^{-3}}$ rise in measured radon concentration (95% CI 0-28%). Refining the analyses to subsets with higher exposure accuracy yielded higher estimates of lung cancer risk. For instance, individuals residing in one or two houses within 5 to 30 years prior to recruitment, with at least 20 years covered by dosimetry, exhibited an 18% increase in lung cancer rate per 100 $\mathrm{Bq\,m^{-3}}$ (95% CI 2-43%). Age, sex, and smoking history did not significantly alter the estimated percentage increase in lung cancer rate per unit increase in measured residential radon concentration beyond what would be expected by chance.

Similar to the European Pooling study, the North American findings supported a linear dose-response relationship with no discernible threshold. However, unlike its European counterpart, formal adjustments for year-to-year variations in residential radon concentrations were not conducted.

The Chinese pooling study

Lubin and colleagues (2004) examined 1,050 cases and 1,996 controls across two studies in Gansu and Shenyang [47]. In pooling the data, they observed a 13% increase in risk per 100 $\mathrm{Bq\,m^{-3}}$ measured radon concentration (95% CI 1-36%). This effect was primarily driven by data from the larger Gansu study. Similar to the European and North American pooling studies, the findings supported a linear dose-response relationship with no identifiable threshold.

Overall evidence on the risk of lung cancer from residential radon

The three major pooling studies examining the risk of lung cancer from residential radon exposure present a consistent picture [1]. They provide compelling evidence that radon is

indeed a cause of lung cancer in the general population, even at concentrations typically found in ordinary homes [1]. Across these studies, there was no significant variation in the proportionate increase in risk per unit increase in radon concentration based on age, sex, or smoking habits of the subjects [1].

Furthermore, the dose-response relationship appears to be linear without a discernible threshold, with substantial evidence indicating an increased risk even at radon concentrations below $200\,\mathrm{Bq\,m^{-3}}$, a threshold commonly advocated for action in many countries [1]. The estimates from these three pooling studies suggest an increased risk of lung cancer ranging from 8% to 13% per $100\,\mathrm{Bq\,m^{-3}}$ increase in measured radon concentration [1]. Combining these estimates the WHO calculated a joint estimate of 10% per $100\,\mathrm{Bq\,m^{-3}}$ [1].

3.3 Radon Origin and Sources

There are different isotopes of radon. In particular, ^{222}Rn, radon-220 (^{220}Rn), and radon (^{219}Rn) are found in natural radioactive chains [48]. Among the naturally occurring radon isotopes, ^{222}Rn and ^{220}Rn have the sufficient half-life (3.8 days and 55.6 s, respectively) to emanate from the rocks and soil into the environment [48]. Because of its short half-life, ^{220}Rn exhibits a smaller diffusion range than ^{222}Rn, thus it is less commonly found in the environment [48]. However, when present, ^{220}Rn can substantially contribute to the overall inhaled dose of radiation [42].

^{222}Rn originates as part of the ^{238}U decay chain and is a direct product of ^{226}Ra decay as shown in Figure 3.1. ^{222}Rn originates from uranium bearing rocks and soils which contain ^{226}Ra. It is then transported to the earth's surface by means of diffusion and convection [49]. Thus, its concentration in the environment depends on the location due to soil type and geology, and atmospheric conditions such as pressure, humidity, wind strength and direction, temperature, snow, precipitation, among others [50].
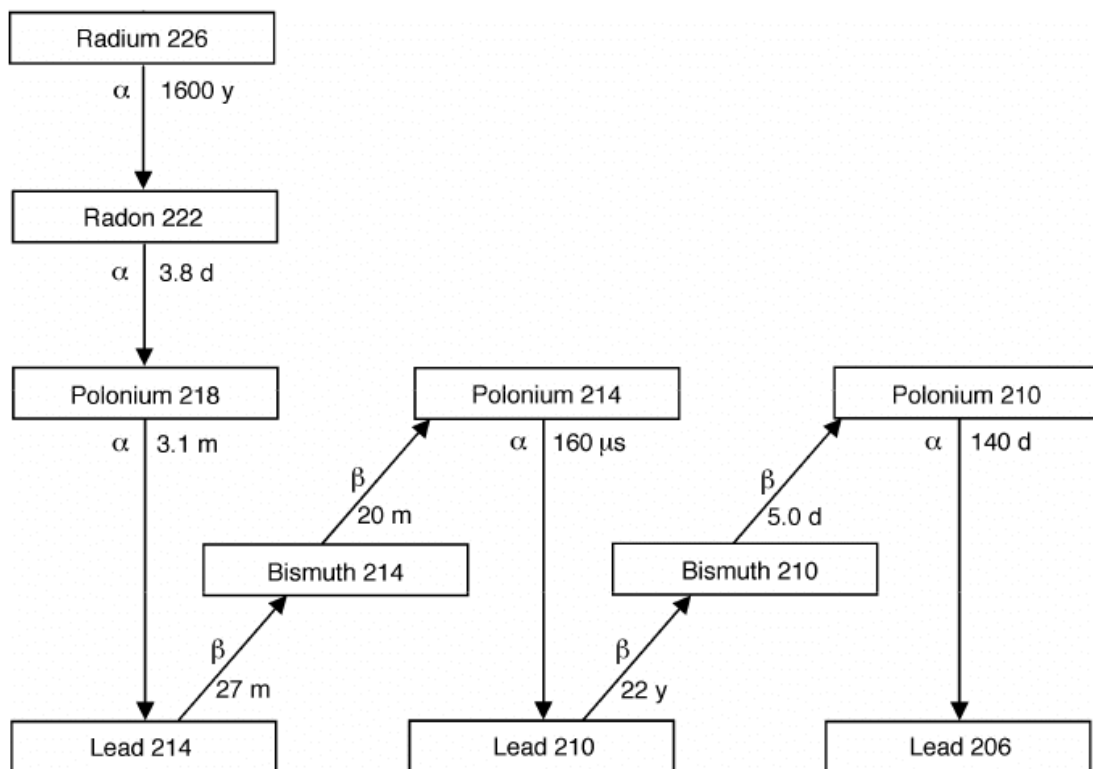
Figure 3.1: Basic ^{222}Rn decay chain. Main decay reactions are shown by arrows with their respective half-life and type of decay. Image created by Gillmore et al [7]. Used under the Creative Commons Attribution 3.0 International License (https://creativecommons.org/licenses/by/3.0/). No changes were made to the image.

Geological events and structures such as telluric movements, faults, and fractures can provide pathways for radon movement from soil to the surface. Additionally, areas with high heat flow and geothermal activity can contribute to increased radon exhalation [51, 52, 53].

3.4   Radon Migration into Buildings

When radon gets to the earth's surface it is rapidly diluted in air [2]. However, it can also enter buildings where it accumulates. It is estimated that in a building approximately 80% of radon comes from the subsoil, 12% from building materials, and less than 1% comes from water [54]. It is important to mention that ^{222}Rn due to its relatively high half-life, is the most representative radon isotope that is found in the environment, so most of the concepts explained in this work are related to ^{222}Rn.

There are different mechanisms and factors influencing radon movement into buildings. Usually, houses have lower pressure than the outside (environment or soil), thus the pressure difference favors radon influx into buildings [8]. Cracks, crevices, and gaps in the infrastructure also provide paths by which radon can enter [8, 2].The pathways by which radon can enter houses are illustrated in Figure 3.2.
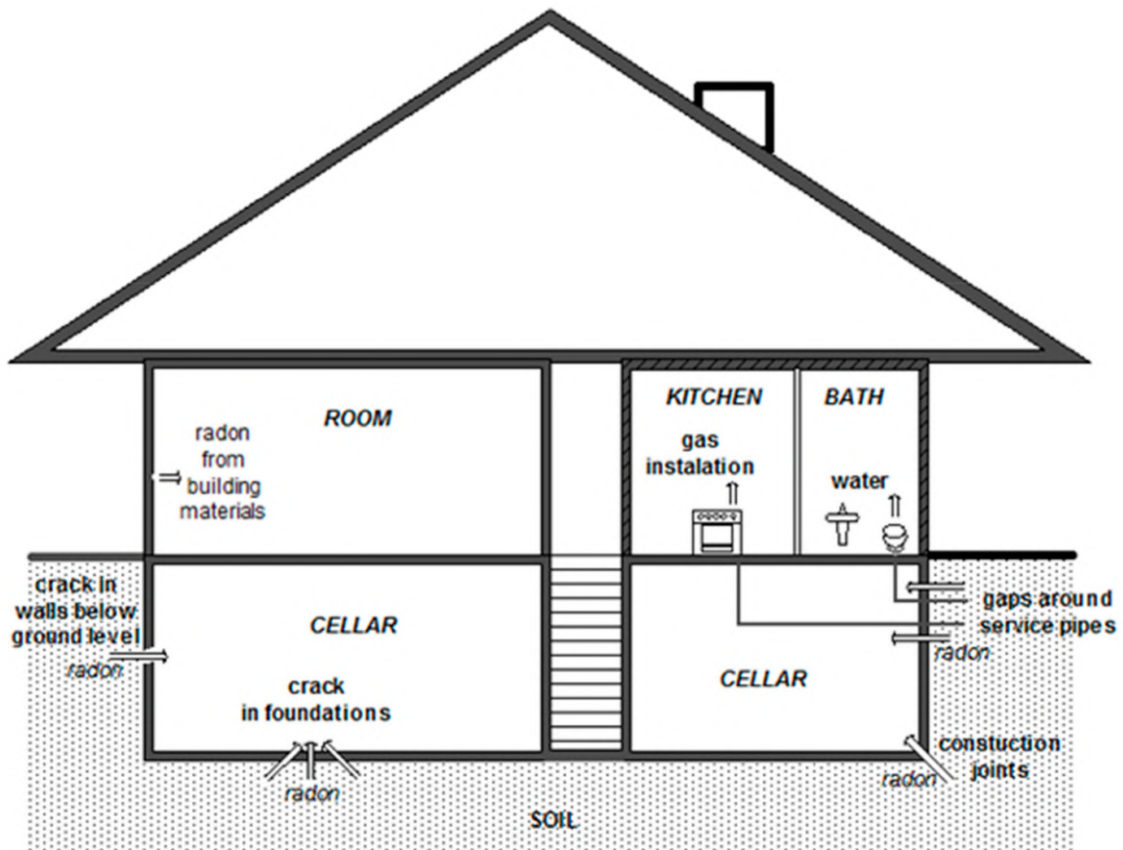
Figure 3.2: Radon pathways into buildings. Image created by Grzywa-Celińska et al [8]. Used under the Creative Commons Attribution 4.0 International License (https://creativecommons.org/licenses/by/4.0/). No changes were made to the image.

Another factor influencing radon levels in houses is temperature [8, 2]. During cold seasons, people tend to keep doors and windows closed, thus radon concentration tends to increase during this period [8]. Indoor temperature and relative humidity also have a relationship with radon concentration [55].

3.5   Radon Exposure Pathways

Radon can get inside the human body through different mechanisms such as inhalation, ingestion, and incorporation through skin [56, 57]. However, it is inhalation what accounts for most of the radon intake [58]. In principle, radon does not pose a human health problem because it is a noble gas and does not chemically react with the constituents of human cells [58]. However, it is its radioactive decay in the respiratory tract and its progeny what represents a problem to human health [58].

^{222}Rn has a short half-life of 3.8 days, and most of its progeny also have a relatively short half-life as can be seen in Figure 3.1 [2]. The progeny formed during the radioactive decay are charged and can aggregate to form clusters that can attach to dust particles in the air. As such, they are called attached fractions [58]. When the attached fraction is inhaled, it can deposit in the airway and deliver large amounts of localized radiation, in particular, alpha particles [58].

The mechanisms by which radon progeny can reach different parts of the respiratory tract can be explained by the mechanisms of deposition particles in the airways [9]. In this sense, the transport of the attached fraction will be directly influenced by the particle size and shape, breathing pattern, ventilation, among others [9]. This process is illustrated in Figure 3.3.

Particles with a diameter of 2-20 µm in the upper respiratory tract (nasopharynx, trachea, and upper bronchi) are affected by inertial momentum and get stuck there, a process known as inertial impaction [59, 60, 61]. Smaller particles (0.1-50 µm) settle due to gravity in the upper respiratory tract, mainly in bronchioles and alveoli, a process known as sedimentation [59, 60, 61]. Diffusion due to Brownian motion increases with decreasing particle size (<0.2 µm) and is predominant in the gas exchange regions of the lung [59, 60, 61].

The unattached progeny (0.5-5 nm) mainly deposits directly after entering the respiratory tract [59, 60, 61]. The deposition pattern is inhomogeneous due to turbulences and inverse flows, causing hot spots of deposition at bifurcations from larger into smaller airways [59, 60, 61]. Particle sizes ranging from 0.2-0.5 µm show a minimal total lung deposition as they are too light for sedimentation but have a decreased diffusion coefficient

due to their size [59, 60, 61].
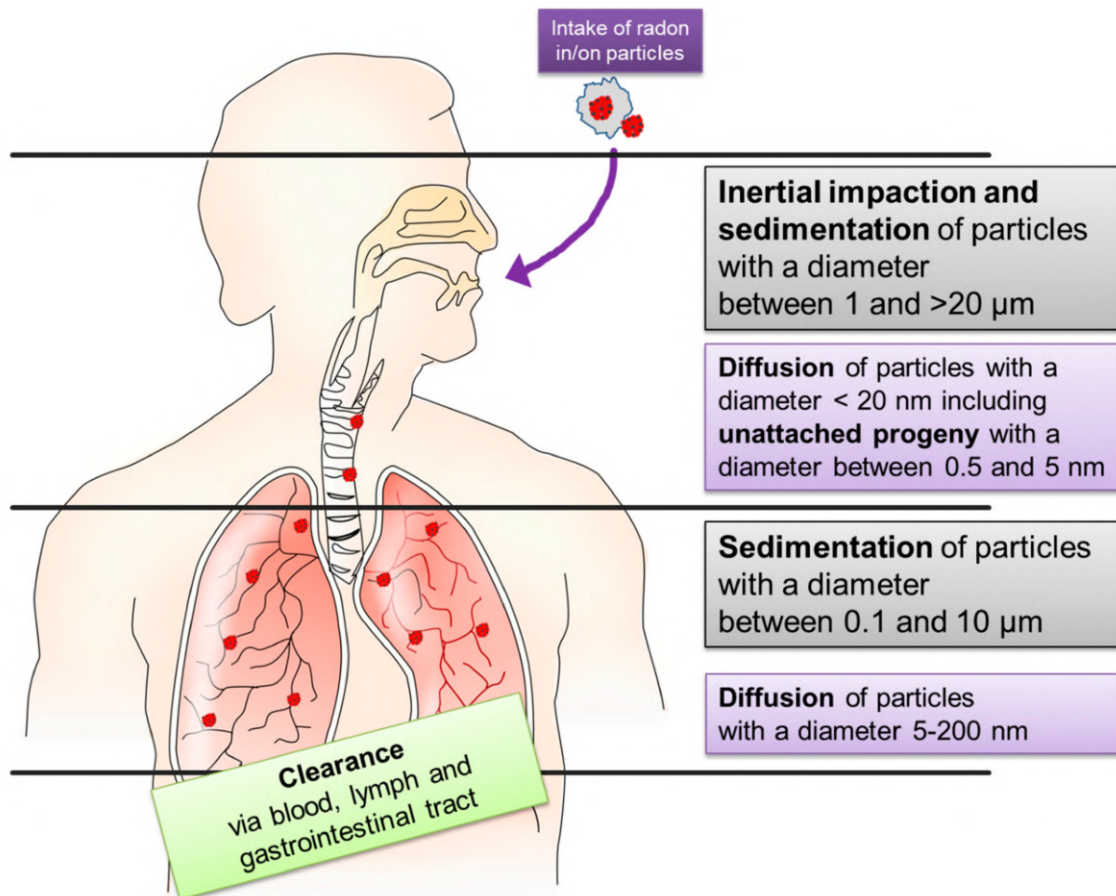
Figure 3.3: Deposition mechanisms of radon progeny. Image created by Maier et al [9]. Used under the Creative Commons Attribution 4.0 International License (https://creativecommons.org/licenses/by/4.0/). No changes were made to the image.

3.6 Radon-Induced Carcinogenesis Mechanisms

According to models and simulations it is estimated that 95% of the total effective dose received by exposure to radon is due to radon progeny, and that less than 5% comes from radon gas [62, 63, 64, 65]. Radiation comes from the radioactive decay of radon and its progeny as shown in Figure 3.1. ^{222}Rn decays into ^{218}Po with the release of high-energy (5.5 MeV) alpha particles. Then, ^{218}Po decays into ^{214}Pb with the release of high-energy (6.0 MeV) alpha particles. Subsequent decays of ^{214}Pb to ^{214}Bi, and ^{214}Bi to ^{214}Po do not significantly contribute to radiation exposure as beta particles have low energy and long range. Decay of ^{214}Po into ^{210}Pb releases high-energy (7.69 MeV) alpha particles [58]. The

following decays of ^{210}Pb, ^{210}Bi, and ^{210}Po are not usually considered as the half-life of ^{210}Pb is 22 years and it is sufficiently long for clearance mechanisms to eliminate it from the body [58]. Table 3.1 shows the energy emissions of the main isotopes in the ^{222}Rn decay series.

Table 3.1: Energy emissions of the main isotopes in the ^{222}Rn decay series [4].

Isotope	Emission energy (MeV)	Decay type
^{222}Rn	5.49	Alpha
^{218}Po	6.00	Alpha
^{214}Pb	0.67, 0.73	Beta
	0.35, 0.30, 0.24	Gamma
^{214}Bi	1.54, 1.51, 3.27	Beta
	0.61, 1.76, 1.12	Gamma
^{214}Po	7.69	Alpha
^{210}Pb	0.06, 0.02	Beta
	0.05	Gamma
^{210}Bi	1.16	Beta
	0.27, 0.30	Gamma
^{210}Po	2.30	Alpha
^{206}Pb		Stable

Exposure to dense ionizing radiation, such as radon alpha particles, can initiate a series of molecular and cellular events that lead to the development of lung cancer [66]. These events include cellular damage, Deoxyribonucleic Acid (DNA) breakage, repair processes, gene mutations, apoptosis, chromosomal changes, genetic instability, and molecular changes in critical regulatory genes [66]. These molecular changes allow cells to escape normal controls and become invasive malignancies [66].

The formation of tumors can begin with DNA damage to cells that have been exposed to radiation [67]. Alpha particles from radiation can cross many individual strands of DNA, causing Multiply Locally Damaged Sites (MLDSs) and producing double-strand breaks, which are the most prominent form of DNA damage [67, 68]. There are two pathways

for repairing double-strand breaks: homologous repair and nonhomologous recombination [67]. In homologous repair, pairing proteins such as rad51 and associated modulatory proteins pair a DNA terminus with the intact DNA homolog, while in nonhomologous recombination, broken DNA ends are rejoined by supporting proteins including Ku70, Ku86, p450 kinase, and DNA ligase IV [67]. The result of DNA breakage and rejoining via the nonhomologous recombination pathway may include some degree of deletion, insertion, or rearrangement of genetic material, which can persist over many cell generations [67, 68].

Ionizing radiation can produce reactive oxygen intermediates that directly affect the stability of the p53 protein, leading to downstream effects on cell regulation and activation of cellular systems sensitive to cellular redox states [69, 70]. Reactive oxygen intermediates can also cause oxidative damage to individual bases in DNA and result in point mutations during DNA replication [70]. The base-excision repair system, involving glycosylases, polymerase β, and ligases, is responsible for repairing this type of damage [70].

The p53 protein plays a crucial role in regulating responses in damaged cells, particularly responses related to cell-cycle arrest and apoptosis [69, 71]. It interacts with other regulatory and repair proteins [69]. When there is cellular damage from direct DNA damage or reactive oxygen intermediates, the lifetime of p53 increases, leading to cell cycle delays and apoptosis [71]. Surviving cells may experience gene deletions, rearrangements, amplifications, and persistent genomic instability [71]. These mutations in oncogenes, loss of function in tumor suppressors, and loss of heterozygosity can contribute to tumor initiation, progression, and invasive malignancy [71]. Thus, the cells that are most likely to result in tumors are those that incur genetic damage or altered genomic stability, not cells that receive lethal damage [71].

Hypomethylation of micro-RNA (miRNA) gene promoters is a mechanism related to radon-induced carcinogenesis. This process leads to a change in the profile of microRNAs, which are small RNA molecules that play a role in gene regulation [10]. In experimental models of radon lung carcinogenesis, microRNAs are massively dysregulated. Initially, these dysregulations are adaptive and aimed at inhibiting neoplastic transformation. However, with long-term exposure to radon, microRNA alterations can lead to the development of cancer [10].

Studies have shown that chronic low-level radon exposure can induce malignant trans-

formation of cells and result in differential expression profiles of microRNAs [72]. Additionally, let-7 microRNA and K-ras have been implicated in radon-induced lung damage both in vivo and in vitro [73]. It is important to note that the underlying mechanisms of radon-induced carcinogenesis are still not fully understood, and further research is needed to fully elucidate the role of microRNAs and other molecular factors in the pathogenesis of radon-induced lung cancer [10]. The mechanisms of radon-induced carcinogenesis are illustrated in Figure 3.4.
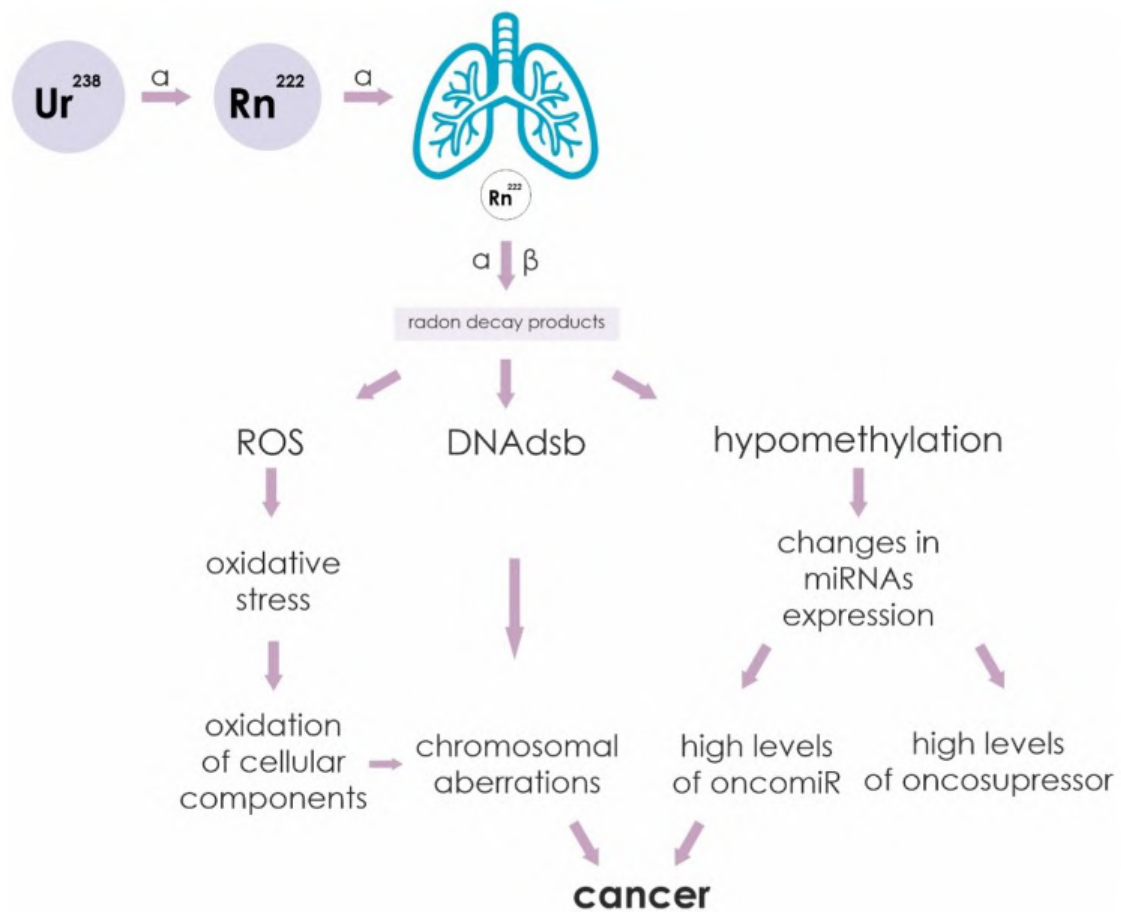
Figure 3.4: Radon-induced carcinogenesis mechanisms. Image created by Pulliero et al [10]. Used under the Creative Commons Attribution 4.0 International License (https://creativecommons.org/licenses/by/4.0/). No changes were made to the image.

3.7   Methods of Radon Detection

Radon measurement in dwellings is a critical aspect of public health due to the potential risks associated with prolonged exposure [1]. Radon measurements are usually discussed in

terms of short-term and long-term measurements [1]. Short-term radon tests can provide an initial estimate of a home's long-term radon concentration [1]. However, these tests can overestimate or underestimate the annual average due to diurnal and seasonal variations, especially during periods when homes are closed or well-ventilated [1]. Therefore, long-term integrated radon measurement devices are preferred for assessing the annual average radon concentration. It is important to note that even yearly radon concentrations can vary within the same home.

Radon levels in homes can vary significantly over time, with fluctuations of 2 to 3 times in a single day and even larger variations from season to season [74]. To accurately determine the annual average radon concentration, it is recommended to conduct long-term measurements lasting 3 to 12 months [74]. During the winter months, when houses are sealed up, higher radon levels are usually observed [74].

Short-term radon tests are designed to monitor the radon levels in a home for a period of 2-7 days [75]. One benefit of short-term radon measurements is that they provide quick results, usually within a week [74, 75, 76]. This can be useful if there is a need to know the radon levels in a home quickly, such as when buying or selling a home [74]. Additionally, short-term tests are less expensive than long-term tests, which can be beneficial in situations of tight budget [74].

Short-term tests can also be used as an initial screening tool to determine if further testing is necessary [74]. If the short-term test indicates high levels of radon, a long-term test can be conducted to confirm the results [75]. Furthermore, short-term tests can be used to investigate the spatial variability of radon concentrations in a home [75]. This can be useful in identifying areas of the home that have higher radon levels than others [74].

A multitude of radon measuring devices exist, each differing in aspects such as design and detection method. Table 3.2 showcases the most commonly used radon measuring devices, as reported by countries participating in the WHO International Radon Project [1]. In particular, passive devices operate without the need for electrical power or a pump in the sampling environment [1]. On the other hand, active devices necessitate electricity and possess the capability to record the variations and levels of radon gas throughout the measurement duration [1].

Table 3.2: Radon gas measurement devices and their characteristics [1].

Detector Type	Passive/ Active	Uncertainty (%)	Sampling Period	Cost
Alpha track detector	Passive	10 - 25	1 - 12 months	Low
Activated charcoal detector	Passive	10 - 30	2 - 7 days	Low
Electret ion chamber	Passive	8 - 15	5 days - 1 year	Medium
Electronic integrating device	Active	≈ 25	2 days - year(s)	Medium
Continuous radon monitor	Active	≈ 10	1 hour - year(s)	High

3.7.1   Alpha Track Detector

Alpha track detectors are a type of passive radon monitoring device that utilizes the damage caused by alpha particles from radon decay to measure the concentration of radon gas [1]. The detector consists of a small piece of specially produced plastic substrate enclosed within a filter-covered diffusion chamber that excludes the entry of radon decay products [1]. When alpha particles are generated by radon or radon decay products in proximity to the detecting material, they can strike the detecting material, producing microscopic areas of damage called latent alpha tracks [1].

The plastic detector material, typically made of polyallyl diglycol carbonate (PADC or CR-39), cellulose nitrate (LR-115), or polycarbonate (Makrofol), is designed to be sensitive to alpha particles but insensitive to humidity, temperature, and background beta and gamma radiation [1]. The alpha tracks are enlarged through chemical or electro-chemical etching of the plastic detector material, making them observable by light microscopy [1]. The number of tracks per unit surface area, after subtracting background counts, is directly proportional to the integrated radon concentration in $Bq\,m^{-3}$.

Figures 3.5 and 3.5 illustrate the various types of alpha track detectors employed in diverse research studies. It is important to note that when the detector is used without a cup or protector, relying solely on the detection film, this configuration is referred to as 'bare mode'.
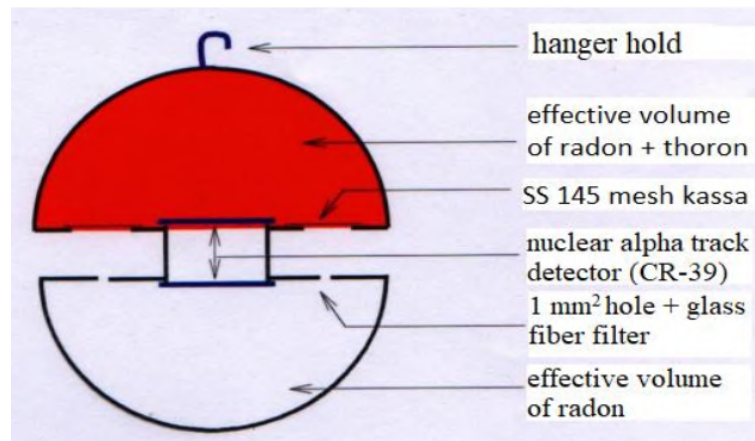
Figure 3.5: Schematic image of alpha track detector. Image created by Wahyudi et al [11]. Used under the Creative Commons Attribution 3.0 International License ((https://creativecommons.org/licenses/by/3.0/). Cropped image.

Figure 3.6: Alpha track detector. Image created by Hassanvand et al [12]. Creative Commons Attribution 4.0 (https://creativecommons.org/licenses/by/4.0/). No changes were made to the image.

3.7.2 Activated Charcoal Adsorption Detector

Activated charcoal adsorption detectors are passive devices used for indoor radon measurement over 1-7 days [1]. They work by adsorbing radon onto activated carbon [1]. After sampling, the detector is sealed, allowing radon decay products to equilibrate with the

collected radon [1]. Gamma counting or liquid scintillation techniques can then analyze the collected radon [1]. Activated charcoal adsorption detectors contain 25 - 90 g of activated carbon for gamma counting or 2 - 3 g for alpha counting [1]. Open-faced or diffusion barrier-equipped canisters can be used to extend the measurement to 7 days [1]. Calibration under various humidity levels and exposure conditions is necessary due to activated charcoal adsorption detectors' sensitivity [1]. Continuous adsorption and desorption by charcoal provide accurate estimates if radon concentration changes are small [1]. Timely analysis is crucial due to radon's 3.8-day half-life [1]. An achievable minimum detectable concentration is around 20 $Bq\,m^{-3}$ for 2 to 7-day exposures [1]. In Figure 3.7 it is presented an schematic representation of a procedure used by Maier et al, to measure radon concentration [13].
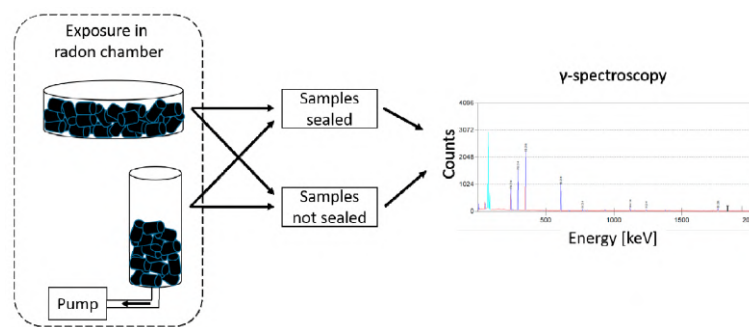
Figure 3.7: Schematic representation of a procedure used to measure radon concentration. Image created by Maier et al [13]. Creative Commons Attribution 4.0 International License (https://creativecommons.org/licenses/by/4.0/). No changes were made to the image.

3.7.3 Electret Ion Chamber

Electret ion chambers are passive detectors used to measure average radon gas concentration over a period [1]. Radon enters the chamber through a filtered inlet, where it ionizes the air, and the ions are collected by a positive electret [1]. The electret discharge over time correlates with radon concentration, measured using a battery-operated reader [1]. Short-term electret ion chambers measure over 2 to 15 days, while long-term ones span 3 to 12 months [1]. Accuracy relies on proper procedures like correcting for background gamma radiation and ensuring electrets are dust-free [1]. In Figure 3.8 it is presented a schematic view of different electret ion chambers [14].
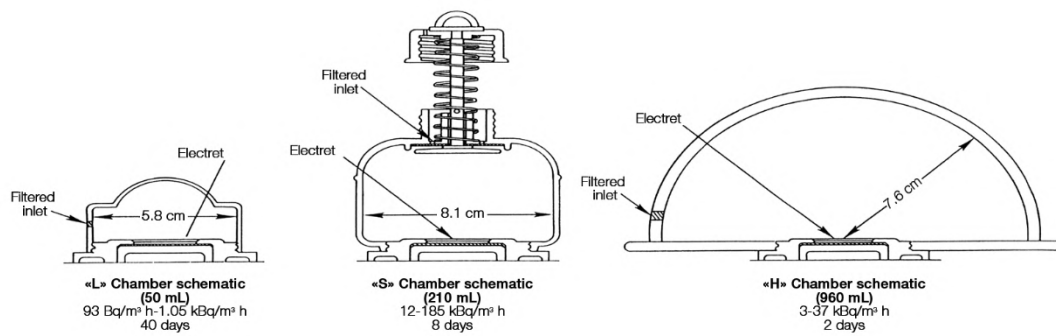
Figure 3.8: Schematic view of different electret ion chambers. Image created by Papastefanou [14]. Used under the Creative Commons Attribution 4.0 International License (https://creativecommons.org/licenses/by/4.0/). No changes were made to the image.

3.7.4 Electronic Integrating Device

Electronic integrating devices are active radon measurement tools that utilize a solid-state silicon detector to track alpha particles emitted from radon decay products, enabling the calculation of average radon gas concentrations over a specified period [1]. These devices offer advantages such as providing time-resolved data on radon concentration fluctuations, shorter measurement periods compared to passive detectors, and a reduced susceptibility to high humidity environments [1]. However, due to their small diffusion chambers, they typically require longer measurement periods for accurate results, usually exceeding two days [1]. Despite this limitation, electronic integrating devices are valuable for their ability to offer detailed and responsive radon data, making them a prominent choice for continuous indoor radon monitoring applications [1].

3.7.5 Continuous Radon Monitor

Continuous radon monitors (CRMs) are sophisticated devices designed to provide real-time, continuous measurements of radon gas levels, typically reporting results in hourly increments [1]. These monitors employ various types of sensors, including scintillation cells, current or pulse ionization chambers, and solid-state silicon detectors, to detect radon [1]. Air is either pumped into a counting chamber or allowed to diffuse into a sensor chamber for analysis [1]. CRMs offer the advantage of providing immediate results upon completion of the test without the need for additional processing [74]. Typically deployed for

a minimum of 48 hours, CRMs are particularly useful for short-term measurement needs such as diagnostic assessments during mitigation processes or initial verification of mitigation success [74]. These devices are equipped with features for storing, displaying, and retrieving logged data, and they often track environmental parameters like temperature, barometric pressure, and relative humidity [74]. Additionally, onboard motion sensors help detect any potential tampering or movement. While CRMs can also perform long-term measurements, their relatively high cost usually limits their use to shorter-term testing applications [74]. Various commercially available CRMs offer unique advantages, such as the capability for alpha spectrometry with solid-state silicon detectors, enabling discrimination between radon and thoron [74]. Some devices address cross-sensitivity to air humidity by incorporating air drying mechanisms [74]. Regular calibration is essential to ensure the accuracy and reliability of CRM measurements [74].

Digital detectors

Digital radon detectors, while not currently recognized by Health Canada due to a lack of formal evaluation, offer convenient and continuous monitoring of radon levels [74]. These detectors resemble consumer-grade carbon monoxide detectors and simply plug into a standard wall outlet [74]. Operating passively, they typically rely on ionization chambers for detection [74]. Some models require a minimum power-on period before displaying concentration readings [74]. These detectors serve both short-term and long-term measurement needs and are particularly popular among homeowners with radon mitigation systems, allowing continuous monitoring within the home environment [74].

However, it is important to note that unlike true continuous radon monitors, these digital detectors lack certain features [74]. They do not offer data downloading or retrieval capabilities, nor do they measure additional environmental parameters beyond radon concentration [74]. Additionally, they may not undergo regular calibration procedures and might not be as sensitive in measuring hourly radon concentrations as CRMs [74]. Despite these limitations, digital radon detectors provide a practical solution for ongoing monitoring needs within residential settings [74].

3.8   Radon Reference Levels

The reference level of radon concentration is a critical benchmark in a country's radon policy [1]. It is the threshold above which remedial actions are strongly recommended or even mandated [1]. The goal is to ensure that radon levels in homes consistently stay below this reference level, and protective measures may be necessary even if the radon concentration is below the reference level [1].

The national reference level signifies the maximum permissible radon concentration in residential dwellings and is a key element of a national program [1]. If a home's radon levels exceed this reference level, remedial actions may be suggested or required [1]. The setting of a reference level should consider various national factors, including radon distribution, the number of homes with high radon levels, the average indoor radon level, and smoking prevalence [1].

The WHO proposes a reference level of $100\,\mathrm{Bq\,m^{-3}}$ to minimize health risks from indoor radon exposure [1]. However, if achieving this level is not feasible due to country-specific conditions, the chosen reference level should not surpass $300\,\mathrm{Bq\,m^{-3}}$ [1]. This upper limit corresponds to approximately $10\,\mathrm{mSv\,y^{-1}}$, as per recent calculations by the ICRP [1].

The ICRP also recommends nations to set radon reference level to As Low As Reasonable Achievable (ALARA) in the range of 100 - $300\,\mathrm{Bq\,m^{-3}}$ [2]. Additionally, in term of effective doses, the recommended levels lie between 3 - $10\,\mathrm{mSv\,y^{-1}}$.

In the United States, the Environmental Protection Agency (EPA) recommends that homes be fixed if the radon level is $4\,\mathrm{pCi\,L^{-1}}$ ($148\,\mathrm{Bq\,m^{-3}}$) or more [77]. However, since there is no known safe level of exposure to radon Americans are advised to fix their home for radon levels between $2\,\mathrm{pCi\,L^{-1}}$ and $4\,\mathrm{pCi\,L^{-1}}$ ($68\,\mathrm{Bq\,m^{-3}}$ and $148\,\mathrm{Bq\,m^{-3}}$) [77]. In Canada and the European Union the reference level are set to $200\,\mathrm{Bq\,m^{-3}}$ [5]. These values are presented in Table 3.3.

3.9   Related Works

Research on measuring radon concentration in dwellings plays a crucial role in understanding the potential health risks associated with this radioactive gas. Various studies have

Table 3.3: Radon concentration guidelines for residential homes [5].

Organization	Residential Level ($\text{Bq}\,\text{m}^{-3}$)
Health Canada	200
World Health Organization	100 - 300
International Commission on Radiological Protection	300
United States Environmental Protection Agency	150
European Union	200

been conducted to assess radon levels in homes and the effectiveness of mitigation strategies. By examining the findings of these studies, we can gain valuable insights into the distribution of radon concentrations, the impact on indoor air quality, and the importance of monitoring and remediation efforts.

A study conducted in Kaya, Burkina Faso, aimed to measure indoor radon levels in residential buildings and estimate the associated doses [78]. Using the Corentium Home digital radon detector, 21 houses were studied over a week-long period. Long-term and short-term values were recorded. Long-term average radon concentrations in residential areas were found to vary between 2.89 and 197.11 $\text{Bq}\,\text{m}^{-3}$. In one house, the annual effective dose was found to be 12 $\text{mSv}\,\text{y}^{-1}$, which is above the recommended levels. The authors recommended implementing radon mitigation techniques to decrease radon concentrations in several houses and called upon authorities to address this issue.

In a study conducted in Koudougou, a city in Burkina Faso, radon concentrations in 24 houses were investigated [79]. The researchers utilized the Corentium Home digital radon detector to record both short-term and long-term values. The long-term radon concentrations ranged from 7.29 to 153.43 $\text{Bq}\,\text{m}^{-3}$. The annual effective doses varied from 0.184 to 3.846 $\text{mSv}\,\text{y}^{-1}$, with an average of 0.972 $\text{mSv}\,\text{y}^{-1}$. Notably, only one house had an annual effective dose of 3.846, which exceeds the standard limits. Based on these findings, the authors concluded that this region of the country is relatively safe in terms of radon exposure.

In another study conducted at Ouagadougou, Burkina Faso, researchers assessed indoor radon concentrations and estimated the annual effective doses [80]. Using the Corentium Home digital radon detector, 21 houses were studied over a week-long period. Long-term and short-term values were recorded. Long-term average radon concentrations in residential

areas were between 4.29 and 114.57 $Bq\,m^{-3}$. The calculated annual effective doses varied between 1.108 and 2.892 $mSv\,y^{-1}$. The authors stated that healthcare authorities should consider indoor radon gas as an important environmental risk factor in Ouagadougou.

In Kirklareli, a city in Turkey, 19 dwellings were studied to measure indoor radon levels [81]. The authors used Corentium Home digital radon detector to record 1-day and 7-days short-term measurements. In the 1-day measurements, the values ranged from 23 to 126 $Bq\,m^{-3}$, and for the 7-days measurements, the values ranged from 16 to 77 $Bq\,m^{-3}$. The annual effective doses ranged from 0.61 to 2.94 $mSv\,y^{-1}$. The authors concluded that the effective doses are below the recommended levels. Additionally, they found that houses with higher indoor radon concentrations are associated with floor level, old construction materials, and rock type.

In a study conducted in the Erzurum province of Turkey, 110 LR-115 detectors were strategically placed in residences throughout the city center and its surrounding areas for an average duration of 60 days [82]. The detectors were installed in frequently occupied rooms such as living rooms and bedrooms to accurately represent the inhabitants' true exposure to radon. The data collected revealed that the average indoor radon concentration did not varied significantly between seasons, with values ranging from 11 ± 6 $Bq\,m^{-3}$ to 380 ± 91 $Bq\,m^{-3}$ in winter, and 8 ± 3 $Bq\,m^{-3}$ to 356 ± 64 $Bq\,m^{-3}$ in summer. The study also calculated the average annual effective dose, which varied from 0.278 $mSv\,y^{-1}$ to 9.59 $mSv\,y^{-1}$ in winter, and 0.202 $mSv\,y^{-1}$ to 8.98 $mSv\,y^{-1}$ in summer. The authors concluded that the calculated doses fall within the 3 - 12 $mSv\,y^{-1}$ range recommended by the ICRP and do not represent a significant health risk.

In a study conducted in Qom, a city in Iran, researchers performed radon measurements in 123 residences [15]. Each dwelling was equipped with a single nuclear alpha track detector, with CR-39 serving as the detector material. The detectors were strategically placed in various parts of the dwellings: in the basement for 35 dwellings, on the ground floor for 40 dwellings, on the first floor for 21 dwellings, and on the second or higher floors for 27 dwellings. This setup was maintained for a period of 90 days. The results revealed that indoor radon concentrations varied between 15 and 259 $Bq\,m^{-3}$. Notably, in 30 residences, which represent 24.3% of the total cases, the radon concentrations exceeded the World Health Organization's recommended level of 100 $Bq\,m^{-3}$. High radon concentration levels

were observed in basements as shown in Figure 3.9. Furthermore, the authors discovered that dwellings with good ventilation generally exhibited lower radon values.
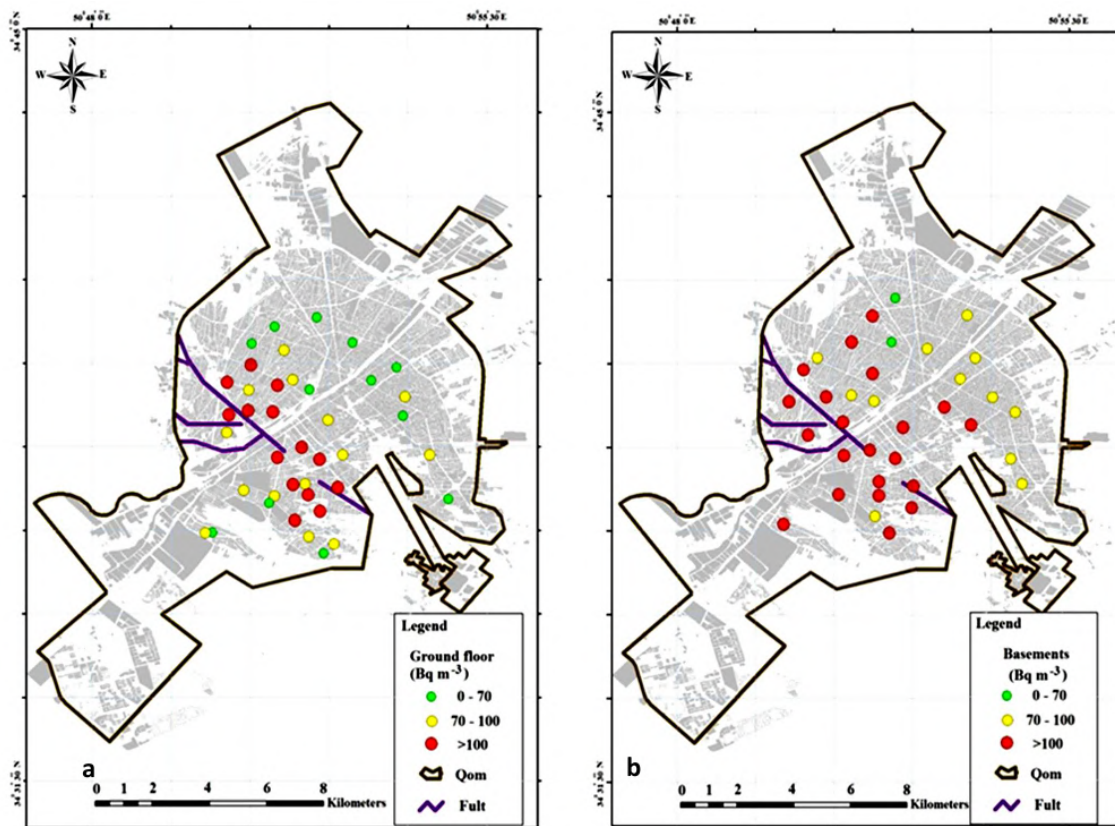
Figure 3.9: Dwellings radon concentration at ground floors (a) and basements (b). Image created by Fahiminia et al [15]. Creative Commons Attribution 4.0 International License (https://creativecommons.org/licenses/by/4.0/). No changes were made to the image.

In a study conducted in Khorramabad, a city in Iran, the indoor radon concentrations of 56 dwellings were examined [12]. The researchers utilized alpha track detectors with CR-39 as the detection material. The results revealed that radon concentrations in the dwellings ranged from 1.08 to 196.78 $\mathrm{Bq\,m^{-3}}$, with an average value of 43.43 ± 40.37 $\mathrm{Bq\,m^{-3}}$. Notably, 10.1% of the dwellings studied, corresponding to six dwellings, exhibited a radon concentration exceeding the 100 $\mathrm{Bq\,m^{-3}}$ limit recommended by the WHO. The researchers calculated the average annual effective dose received by the residents of the studied area to be 1.09 $\mathrm{Bq\,m^{-3}}$. Approximately 7.1% of the samples, corresponding to four dwellings, had an annual effective dose exceeding 3 $\mathrm{Bq\,m^{-3}}$. The study found that radon concentrations were higher in houses compared to apartments. Figure 3.10 displays the distribution map of indoor radon in Khorramabad.
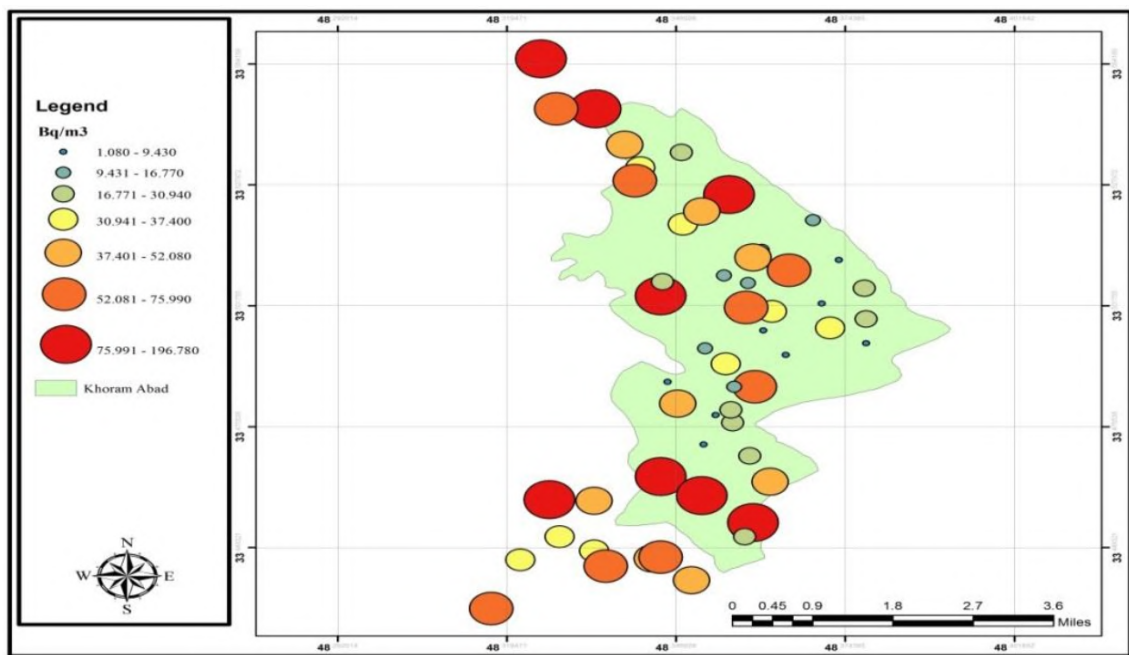
Figure 3.10: Distribution map of indoor radon in Khorramabad. Image created by Hassanvand et al [12]. Creative Commons Attribution 4.0 International License (https://creativecommons.org/licenses/by/4.0/). No changes were made to the image.

In a study conducted on Madura Island, Indonesia, an indoor radon survey was performed [11]. Initially, the island was systematically sampled using a grid system measuring 20 km x 20 km. On each grid, 5 to 10 alpha track detectors, with CR-39 as the detecting material, were placed for a duration of 3 to 4 months. In total, 95 detectors were strategically positioned across 13 areas of the Madura Islands. The indoor radon concentrations in these 13 areas varied from 15.11 ± 1.07 Bq m^{-3} to 126.93 ± 8.98 Bq m^{-3}, with an average concentration of 58.74 ± 4.15 Bq m^{-3}. The authors concluded that the indoor radon concentrations were below the limits set by the ICRP. Utilizing this data, they constructed a radon distribution map which is shown in Figure 3.11.
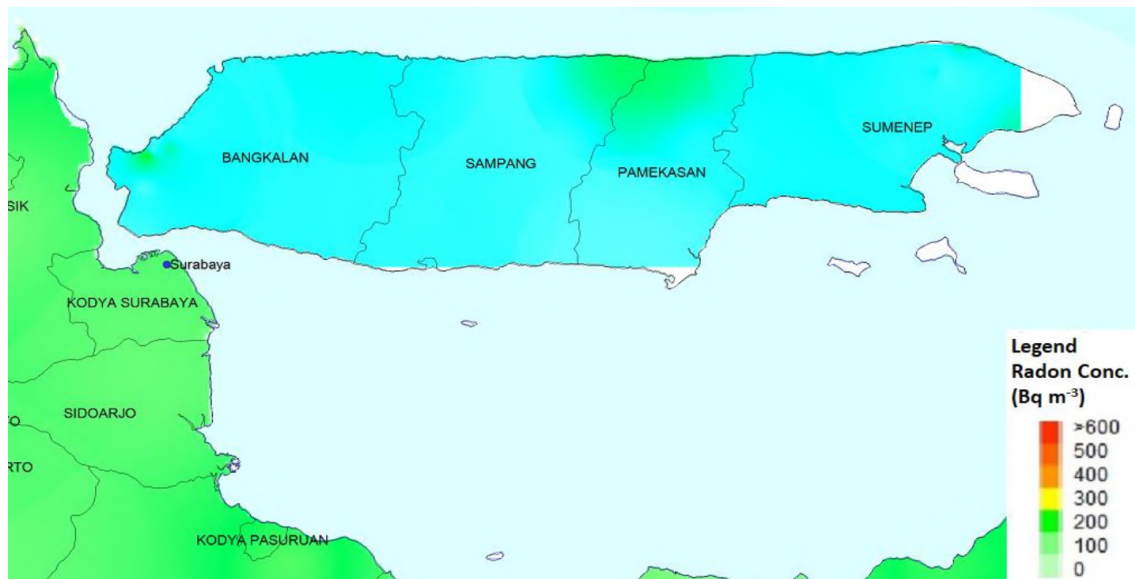
Figure 3.11: Map of the indoor radon concentration in Madura dwellings. Image created by Wahyudi et al [11]. Used under the Creative Commons Attribution 3.0 International License (https://creativecommons.org/licenses/by/3.0/). No changes were made to the image.

In a study conducted in Lima, Peru, researchers investigated radon concentrations in four districts: Lima Centro, Lima Este, Lima Norte, and Lima Sur [83]. The researchers sampled each district using a 5 km x 5 km grid system, placing detectors based on the population density within each grid. The minimum number of sampled dwellings was determined by the population: zero for less than 2,500, one for less than 5,000, two for less than 10,000, four for less than 20,000, and six for more than 20,000. A total of 508 dwellings were studied using 508 alpha track detectors with LR-115 as the detection material in bare mode. The results showed that 88.9% of the dwellings had radon levels below 100 $\mathrm{Bq\,m^{-3}}$, 9.84% had levels between 100 and 200 $\mathrm{Bq\,m^{-3}}$, and 1.18% had levels higher than 200 $\mathrm{Bq\,m^{-3}}$. The concentration of radon was closely related to the zones, as evidenced by a strong correlation with geological characteristics. It was also related to other variables such as the age of construction. This factor seems to indicate that proper maintenance of dwellings (without cracks or fissures) contributes to lower levels of radon inside dwellings. The authors concluded that the detected levels do not pose a high risk to the population, since the average radon concentration values were below the reference level suggested by the WHO.

In a study conducted in Beijing, China, indoor radon levels were examined in 800

dwellings [84]. The researchers utilized 800 alpha track detectors, equipped with radon cups and CR-39 as the detection material. These detectors were deployed for a period of one year. The results revealed that the radon concentrations in the dwellings varied from 12.1 ± 2.5 to 119.0 ± 7.8 Bq m^{-3}. Interestingly, only one dwelling, representing 0.13% of the total dwellings studied, had an annual average radon concentration exceeding 100 Bq m^{-3}. The annual geometric mean of radon concentration was found to be 39.3 ± 12.9 Bq m^{-3}, while the arithmetic mean was 42.0 ± 13.7 Bq m^{-3}. The authors observed that radon levels were higher on the ground floor compared to the upper floors. However, no significant difference was noted among the upper floors. Additionally, the authors suggested that the radon levels on the upper floors could be attributed to the building materials used.

Research on measuring radon concentration in dwellings is critical for understanding the potential health risks associated with this radioactive gas. Various studies have been conducted globally to assess radon levels in homes and evaluate the efficacy of mitigation strategies. Table 3.4 offers a comprehensive overview of these studies, presenting key findings such as ranges of radon concentrations, sample sizes, and details on measurement methods and duration.

Table 3.4: Summary of studies on indoor radon levels in residential dwellings: locations, sampling details, measurement duration, measuring devices, and results. Note: 'avg.' denotes average.

Location	Sample	Measuring Device	Measurement Duration (Days)	Radon Levels (Bq m^{-3})	Reference
Kaya (Burkina Faso)	21	Corentium Home	7	2.89 - 197.11 (avg. 28.47)	[78]
Koudougou (Burkina Faso)	24	Corentium Home	7	7.29 - 153.43	[79]
Ouagadougou (Burkina Faso)	21	Corentium Home	7	4.29 - 114.57 (avg. 26.90)	[80]
Kirklareli (Turkey)	19	Corentium Home	7	16 - 77 (avg. 40.8)	[81]
Erzurum (Turkey)	110	Alpha track detector with LR-115	60	11 - 380	[82]
Qom (Iran)	123	Alpha track detector with CR-39	90	15 - 259	[15]
Khorramabad (Iran)	56	Alpha track detector with CR-39	60 - 90	1.08 - 196.78 (avg. 43.43)	[12]
Madura Island (Indonesia)	95	Alpha track detector with CR-39	90 - 120	15.11 - 126.93 (avg. 58.74)	[11]
Lima (Peru)	508	Alpha track detector with LR-115	56 - 84	15 - 306 (avg. 49)	[83]
Beijing (China)	800	Alpha track detector with CR-39	365	12.1 - 119.0 (avg. 42.0)	[84]

From Burkina Faso to China, researchers have employed an array of techniques, from Corentium Home digital radon detectors to alpha track detectors with CR-39 and LR-115 detection materials, to assess radon levels over varying locations. The findings underscore the variability in radon concentrations, ranging from relatively low levels to instances where concentrations exceed recommended limits, indicating potential health risks. Additionally, the studies reveal correlations between radon levels and factors such as geographic location, construction materials, and ventilation. Understanding these nuances is pivotal in formulating effective mitigation strategies and regulatory measures to safeguard public health from the adverse effects of indoor radon exposure.

3.10   Radon Studies in Ecuador

Despite the health problems that radon can pose to human health, public general knowledge about this topic is scarce in many countries [85, 86, 87, 88, 89]. In Ecuador some studies have been performed regarding radon levels in different contexts. A study conducted in the Jumandy cave in the Amazon region of Ecuador aimed to assess the concentrations of radon ^{222}Rn and its potential health risks [90]. This study is significant as it is one of the few radioactivity studies performed in Latin America and the first in the Andean Mountains. The study found that the highest average concentration of ^{222}Rn was observed at the cave entrance, reaching 1,381 Bq m^{-3}. This high concentration was attributed to the ventilation effect, with wind potentially transporting ^{222}Rn from the inside of the cave. Additionally, the study identified the highest concentration peaks of ^{222}Rn deep within the cave, reaching 4,100 Bq m^{-3} during the wet season. These peaks were attributed to a drop in temperatures.

In a study conducted in major cities of the province of Chimborazo, in the central Andes of Ecuador, researchers evaluated ^{222}Rn radioactivity in 53 public water sources, including underground and surface waters, across five geological zones [91]. The Pisayambo Volcanic unit exhibited the highest radon concentration (9.58 ± 3.04 Bq m^{-3}), while surface waters showed no radon activity. Despite variations, all detected radon levels were below recommended limits for human use. Maximum annual effective radiation doses from radon ingestion and inhalation also remained within safe ranges for the population across different

cities. The study additionally established a correlation between ^{222}Rn activity and the parent isotope ^{226}Ra in certain spring samples.

Another study examined the presence of radon gas in construction materials such as clay and sand from the Palopo mining area in Latacunga [92]. Emanation values were for clay ($29.7213\,\mathrm{Bq\,m^{-3}}$) and ($0.6769\,\mathrm{Bq\,m^{-3}}$) for sand. Physical properties like particle size and humidity influenced the gas release. Artisanal brick factories showed levels within limits: $(0.079 \pm 0.031)\,\mathrm{Bq\,m^{-2}h^{-1}}$ for factory 1, $(0.149 \pm 0.046)\,\mathrm{Bq\,m^{-2}h^{-1}}$ for factory 2, and $(0.124 \pm 0.068)\,\mathrm{Bq\,m^{-2}h^{-1}}$ for factory 3. Population exposure through constructions using these bricks resulted in $(2.168 \times 10^{-3}\,\mathrm{mSv\,year^{-1}})$, well below the $(1.1\,\mathrm{mSv\,year^{-1}})$ limit. In summary, clay bricks do not pose a radiological risk due to radon exhalation.

According to a study the mean radon concentration in Ecuador ranges from 20.39 to 225.66 $\mathrm{Bq\,m^{-3}}$ and an average of 94.30 $\mathrm{Bq\,m^{-3}}$ [19]. However, in the study only 61 houses located in Quito were studied, so more studies regarding radon levels in Ecuador are needed.

Measurements of radon concentration were conducted in residential, office, and university laboratory settings within Riobamba city [93]. The analysis encompassed various parameters such as building materials, age, and occupancy patterns. Employing a Corentium Home digital radon detector capable of providing both 24-hour and 7-day readings, the research shed light on the radioactive radon levels. Encouragingly, the findings indicate that the radon concentrations in both residential and occupational spaces in Riobamba remain within the safety thresholds recommended by the WHO. However, it is noteworthy that the absence of localized regulations for natural radioactive elements in Ecuador and the wider region necessitates reliance on international standards. Most of the examined structures demonstrated radon levels closely resembling the approximately 16 $\mathrm{Bq\,m^{-3}}$ outdoor environmental concentration in the region. Notably, older constructions with less effective floor sealing exhibited slightly elevated radon levels, though still compliant with international guidelines. Interestingly, middle-aged buildings with modern, airtight flooring and multiple layers of paint presented lower radon concentrations in comparison to new houses.

For his undergraduate thesis project Marlon Loayza created a radiological map of the Radon levels in the homes of the urban parishes of the city of Cuenca, Ecuador [94]. The

map was designed based on Radon concentrations obtained from the sampling of 47 homes, distributed among the different urban parishes of the city of Cuenca. Solid detectors of nuclear traces LR 115 type 2 (cellulose nitrate) were used for the sampling, placed in naked mode and at an average height where breathing occurs according to the sector of the house. The kitchen was sampled at a height of between 1 and 2 m, while the bedroom was sampled at a height of between 0.5 m to 1 m. The data obtained after 2 samplings (at intervals of 45 days) registered minimum Radon concentrations of 8.33 $\mathrm{Bq\,m^{-3}}$ and maximum of 148.33 $\mathrm{Bq\,m^{-3}}$ with an average of 35 $\mathrm{Bq\,m^{-3}}$.

In his undergraduate thesis project, Bruno Castillo measured radon concentrations in preschool classrooms in Cuenca [95]. The investigation covered 32 classrooms in both urban and rural areas, shedding light on radon's potential health implications. The measured average radon concentration of 20.03 $\mathrm{Bq\,m^{-3}}$ fell comfortably below intervention limits, suggesting a generally safe environment in these educational spaces. Beyond radon levels, the study probed the link between building characteristics and radon concentrations. Surprisingly, no significant associations were found between these variables and the observed radon levels. This outcome emphasizes the need for more in-depth analysis to uncover the precise sources of radon within the classrooms. Additionally, the research delved into radiation exposure, finding that the annual absorbed dose was 0.2526 $\mathrm{mSv\,y^{-1}}$, and the annual effective dose was 0.6063 $\mathrm{mSv\,y^{-1}}$.

Chapter 4

Methodology

4.1 Methodology Graphical Abstract

Figure 4.1 provides a graphical abstract summarizing the methodology employed in this study.
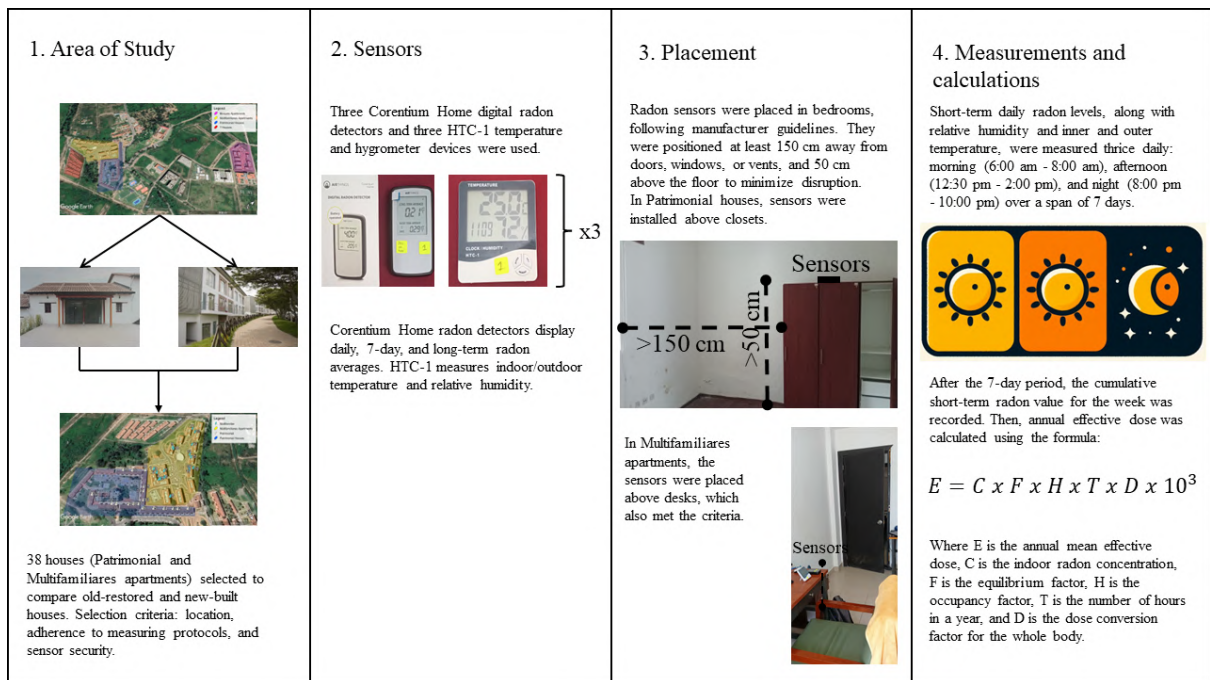
Figure 4.1: Graphical abstract of the methodology used.

4.2   Description and Delimitation of the Area of Study

San Miguel de Urcuquí is a town located in Imbabura province, Ecuador. Yachay Tech University is a public university in San Miguel de Urcuquí. Yachay Tech, is closely tied to the historical evolution of the land it now occupies [16]. The university's location has a rich history as it was once part of a sprawling hacienda known as San Jose [16]. Initially, this hacienda spanned an impressive 872 hectares and held prominence as the largest and most extensive land in the Urcuquí town [16].

Its origins trace back to the ownership of the Jesuits, but over time, it passed into the hands of various notable figures [16]. General Juan José Flores, the first Constitutional President of the Republic of Ecuador, was among its early owners [16]. Subsequently, the property changed hands to Don Jacinto Jijón and Caamaño y Flores, a historian, leader of the extinct Conservative Party, and a significant player in the sugar industry during the 1920s [16]. The hacienda's legacy continued with its last recorded owner, Mr. Francisco Salvador [16].

Today, the San Jose hacienda has transformed into the central administrative hub of Yachay Tech within the broader Yachay City project [16]. This visionary urban area prioritizes research and technological applications, all aimed at realizing the concept of Good Living [16]. Yachay City operates as an innovation-driven ecosystem that fosters and amplifies technology-based enterprises [16]. It is a dynamic space where academia, research, and cutting-edge innovation converge to shape the future [16].

Due to its history, Yachay Tech University's campus comprises a blend of buildings with different origins – some have been restored and readapted from existing structures, while others are newly constructed [16]. The Ingenio Azucarero is an example of restored and repurposed structure, it is depicted in Figure 4.2. This historical site once operated as a sugar mill but has been transformed into a museum showcasing the machinery once used for processing sugar cane [16]. Additionally, another part of the site now accommodates administrative offices and Yachay Tech's library [16].

(a)   (b)

Figure 4.2: (a) Ingenio Azucarero in the past, (b) Restored and readapted Ingenio Azucarero. Images taken from Yachay Tech University's web page [16].

Another example is the Sala Capitular, which is depicted in Figure 4.3. The Sala Capitular served as a religious chapel for the workers of the hacienda, now it is used for meetings and lectures [16].

(a)   (b)

Figure 4.3: (a) Sala Capitular in the past, (b) Restored and readapted Sala Capitular. Images taken from Yachay Tech University's web page [16].

Yachay Tech campus is a residential campus, students can choose to live in one of the four types of housing: Apartments – Bloques, Apartments – Multifamiliares, Patrimonial Houses, and Patrimonial T Houses [96]. In Figure 4.4, it is shown a map of Yachay Tech university in which it is highlighted the zones of the four types of houses.

Figure 4.4: Yachay Tech University map highlighting the location of the four types of houses. In purple Bloques apartments, in yellow Multifamiliares apartments, in red T houses, and in blue Patrimonial Houses. Image created with Google Earth Pro V7.3.6, imagery date 26/11/2021, coordinates: 0°24'06.43" N 78°10'28.02" W.

Among the four types of houses on the Yachay Tech campus, the Patrimonial houses stand out due to their unique characteristic of being restored and readapted, as illustrated in Figure 4.5. In contrast, the other types of buildings were constructed along with the university buildings.

(a)   (b)

Figure 4.5: (a) Patrimonial houses in the past, (b) Restored and readapted Patrimonial houses. Images taken from Yachay Tech Library.

In this study, we aim to investigate and compare radon concentrations between two distinct categories of houses: old-restored houses and new-built houses. Patrimonial houses

represent the old-restored houses group, while Multifamiliares apartments were chosen as the new-built houses group due to is proximity to Patrimonial houses, see Figure 4.6.

Figure 4.6: Multifamiliares apartments. Images taken from Yachay Tech University's web page [16].

In this study, 36 houses were studied, 18 Patrimonial houses and 18 Multifamiliares apartments. The houses were chosen based on the following criteria:

(i) Location: Sensors were strategically positioned to encompass the maximum area of houses.

(ii) Commitment to adhere to sensor protocols: The sensors need to meet specific criteria and positional standards to ensure their proper functioning.

(iii) Security of the devices: The sensors were placed in houses where device integrity could be ensured.

The final distribution of the houses to be studied is shown in Figure 4.7. Yachay Tech has its own system to name their houses, however, for simplicity a label from 1 to 18 was given for each type of house.

Figure 4.7: Yachay Tech University map highlighting the two types of houses that were studied for radon levels. In yellow Multifamiliares apartments zone and in blue Patrimonial houses zone. A white pin indicates the Patrimonial house studied and assigns a label from 1 to 18. A light blue pin indicates the Multifamilares apartment studied and assigns a label from 1 to 18. Image created with Google Earth Pro V7.3.6, imagery date 26/11/2021, coordinates: 0°24'06.43" N 78°10'28.02" W.

4.3 Data Collection

4.3.1 Sensors

Radon sensor

In this study, three digital radon detectors were used, specifically the Corentium Home by Airthings. The Airthings Corentium Home detector uses a passive diffusion chamber to allow air samples to flow into it [97, 98]. The radon sensor in the device uses alpha spectrometry to measure the level of radon [97, 98]. The sensor consists of a photodiode located inside the chamber, which counts the amount of daughter radon particles in the air sample [97, 98]. The device is calibrated to detect alpha particles emitted by the radioactive gas radon, and the photodiode is designed to only register relevant particles [97, 98]. The device analyzes air in 30-minute increments, using just 25 cm^3 to analyze the entire room [97, 98]. The sensor counts events continuously and keeps a ledger of these counts on an

hourly basis [97, 98]. To calculate the actual radon concentration, a new calculation runs every hour and includes the counts for the past 24 hours, resulting in a new update to a 24-hour average [97, 98].

Radon measurement differs from instant measurements such as temperature [97, 98]. Instead of immediate readings, radon is gauged as an average value. In practical terms, the sensor tallies the alpha particles from radon in each air sample it examines [97, 98]. The detector operates non-stop, generating a data point every hour that adds to an overall reading [97, 98]. Consequently, radon levels are typically presented as averages spanning periods like 24 hours, 48 hours, a week, a month, and so on [97, 98]. The Corentium Home radon detector gives the following readings [99]:

(i) Short-term average - 1-day (last 24 hours) - Updated Hourly: The short-term average over a 1-day period, which represent the most recent 24 hours, is subject to hourly updates. This particular average offers a preliminary estimate of the radon concentration within the defined time frame. However, it is essential to recognize that this approximation comes with inherent limitations in terms of accuracy as radon concentration can vary from day-to-day and may not reflect the real radon concentration. Consequently, it is not advisable to use this 1-day average as the sole basis for making decisions regarding necessary remediation actions.

(ii) Short-term average – 7-days (updated daily): An additional short-term average is computed over a duration of 7 days and receives daily updates. It is important to take into account that this 7-days average becomes available only after the monitoring device has accumulated data over a full week. This average is then refreshed once every day.

(iii) Long-Term Average - cumulative measurement period: The long-term average, in contrast, is derived from continuous measurements spanning the entirety of the device's current monitoring period. For a long-term measurement to yield significant and reliable results, it is recommended to let the measurement device operate continuously for a minimum of 30 days. This extended duration is crucial for obtaining an accurate representation of radon levels over time.

Table 4.1: Corentium Home radon detector technical specifications.

Operation environment	Temperature: +4 °C to +40 °C Relative Humidity: <85 %
Measurement range	Lowest detection limit: $0\ \mathrm{Bq\,m^{-3}}$ Upper display limit: $9999\ \mathrm{Bq\,m^{-3}}$
Accuracy/precision at $200\ \mathrm{Bq\,m^{-3}}$	7 days: 10 % 2 months: 5 %

Figure 4.8 shows the radon detector used in this study. The measurement units in this device are $\mathrm{pCi\,L^{-1}}$, but measurements were transformed into SI official units $\mathrm{Bq\,m^{-3}}$. According to the manufacturer's user manual, the technical specifications for this device are listed in Table 4.1.

Figure 4.8: Corentium Home radon detector. Photo taken by author.

Inner temperature and relative humidity sensor

HTC-1 device was used to measured temperature and relative humidity, a photo of the device is shown in Figure 4.10. Temperature measurements were taken in Celsius degrees and relative humidity was measured in percentages. The manufacturer's technical specifications for the device are shown in Table 4.2.

Figure 4.9: HTC-1 thermometer and hygrometer device. Photo taken by author.

Table 4.2: HTC-1 technical specifications.

Temperature measurement range	-10 °C ∼+50 °C
Temperature measurement accuracy	± 0.1 °C
Humidity measuring range	10 % ∼99 % RH
Humidity measuring accuracy	± 5 % RH

4.3.2   Protocol

Time of study

The study was conducted within specific time constraints, which influenced the design and scope of the research. Due to limited availability of Corentium Home digital radon detectors, measurements were conducted for seven days, plus an additional initial day for setup and data collection.

As the study was conducted within Yachay Tech's campus residences, access to the houses was only possible during class periods. Furthermore, an unforeseen delay occurred at the beginning of Yachay Tech Semester II 2022, resulting in the closure of most Patrimonial houses. Permissions were subsequently obtained to access these houses, leading to measurements being conducted in two separate periods.

The Patrimonial houses were studied from November 7, 2022, to March 20, 2023, while the Multifamiliares apartments were studied from April 17 to June 15, 2023. Measurements were not carried out during extended holiday periods, specifically from December 24, 2022, to January 2, 2023, and during the end-of-semester break from March 21 to April 16, 2023, due to difficulties in access or data retrieval from the deployed detectors.

Placement

The radon sensor was placed in a living area, such as a bedroom, where sunlight and moisture do not reach the device, following the manufacturer's recommendation. The device was placed at least 150 cm from the nearest door, window, or air vent, and 50 cm above floor level. The measurement location was selected with the reasonable expectation that the measurement device would not be disturbed during the measurement period. The HTC-1 device was placed next to the radon sensor.

All Patrimonial houses are equipped with closets of the same model, see Figure 4.10. Thus, sensors were placed above them. This complies with the radon detector manufacturer's recommendations. During the time lapse of the study, all studied Patrimonial houses were uninhibited because they required maintenance. In Multifamiliares apartments, sensors were placed on desks that also met the manufacturer's recommendations as shown in Figure 4.11.
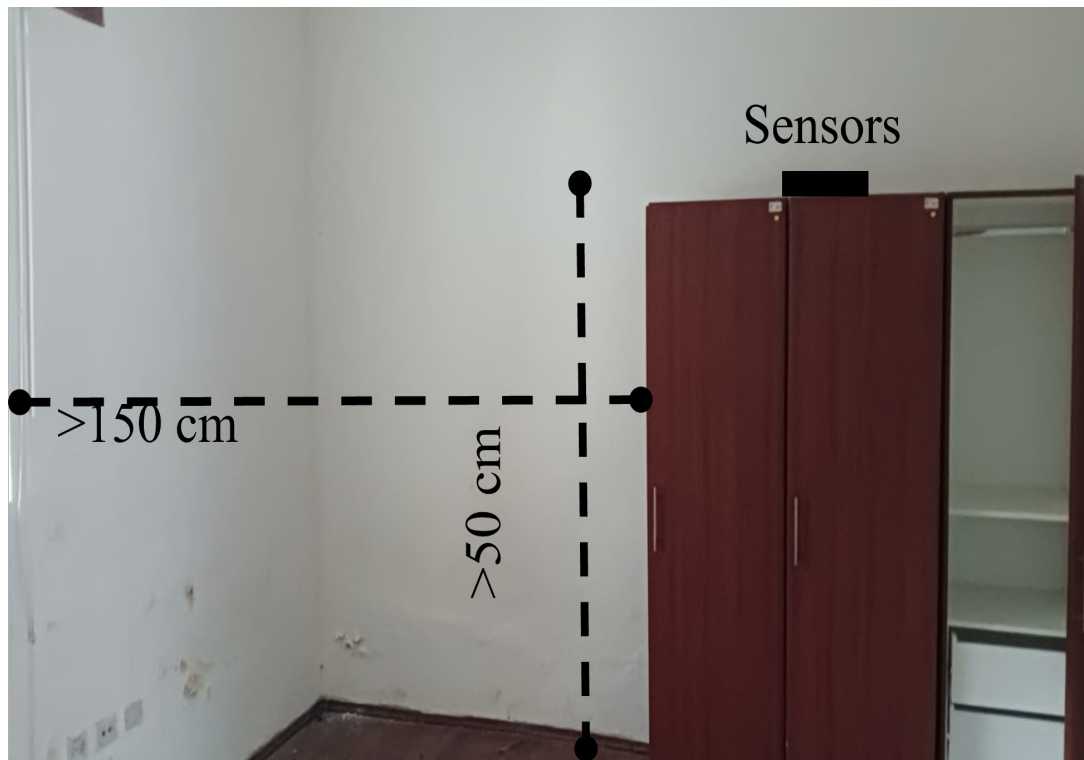
Figure 4.10: Placement of detectors above closet in Patrimonial house. Photo taken by author.

Measurements

During a 7-day period, short-term 1-day radon concentration, inner temperature, and relative humidity were recorded three times per day (morning, afternoon, and night). Morning was defined as 6:00 am - 8:00 am, afternoon was defined as 12:30 pm - 2:00 pm, and night was defined as 8:00 pm - 10:00 pm. It is worth noting that the first day of each measurement period was considered an extra day to allow the device to analyze air samples, with readings beginning the next morning after device setup.

After 7 days, the radon detector displayed the short-term 7-day value, which was also recorded. The values were recorded on-site by the author or requested from students housing the detectors, as illustrated in Appendix Figure 1.
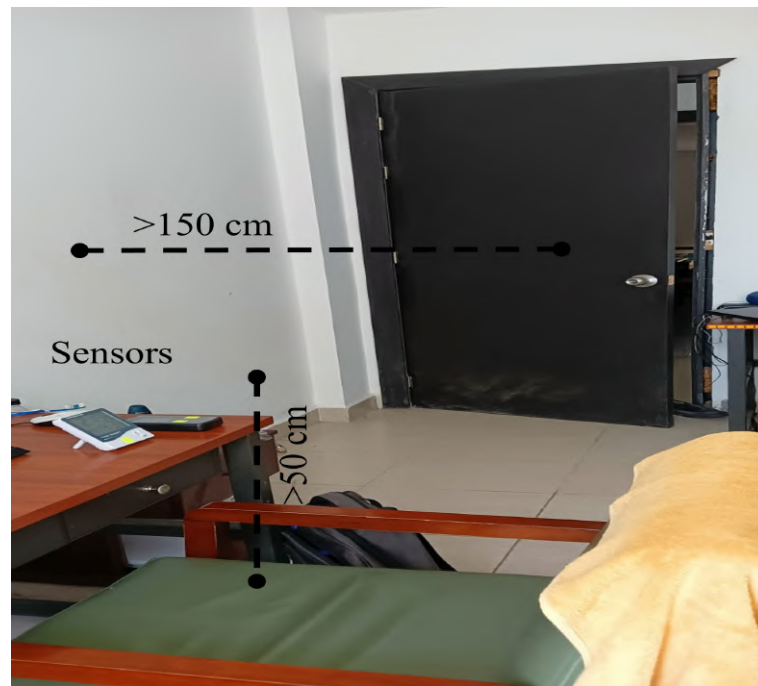
Figure 4.11: Placement of detectors on desk in Multifamiliares apartment. Photo taken by author.

4.4   Annual Effective Dose Calculation

To calculate the annual effective dose resulting from indoor radon exposure, equation 4.1 was used. This equation, which has been employed in previous studies [100, 101], allows for the estimation of the dose based on specific factors and variables. By applying this equation, it becomes possible to assess the potential health risks associated with indoor radon concentrations [54].

$$E = C \times F \times H \times T \times D \times 10^3 \tag{4.1}$$

Where E is the annual mean effective dose (mSv y^{-1}) due to indoor radon, C is the indoor radon concentration (Bq m^{-3}), F is the equilibrium factor (0.4 for indoor measurements), H is the occupancy factor (0.8 for indoor measurements), T is the number of hours in a year (8760 hours for one year of residence in the house), and D is the dose conversion factor for the whole body dose calculation (9 nSv (Bq h m^{-3})$^{-1}$).

Chapter 5

Results and Discussion

5.1 Short-Term Radon Variability: Daily Averages

The short-term variability of radon levels was examined through daily average measurements taken at three intervals: morning, afternoon, and night, over a period of seven days in 36 selected houses. To illustrate these findings, bar plots were generated for each house, displaying the daily radon measurements.

In each graph, the morning measurements are represented in yellow, afternoon in orange, and night in blue. A black line denotes the median value for each day, aiding in the visualization of central tendencies. Additionally, a horizontal red line at $100 \, \mathrm{Bq \, m^{-3}}$ is drawn to indicate the reference level recommended by the WHO.

Additionally, to facilitate comparison, all graphs maintain a consistent height scale, allowing for easy visual assessment.

5.1.1 Patrimonial Houses

The plots representing short-term daily values for Patrimonial houses are presented in Figure 5.1.
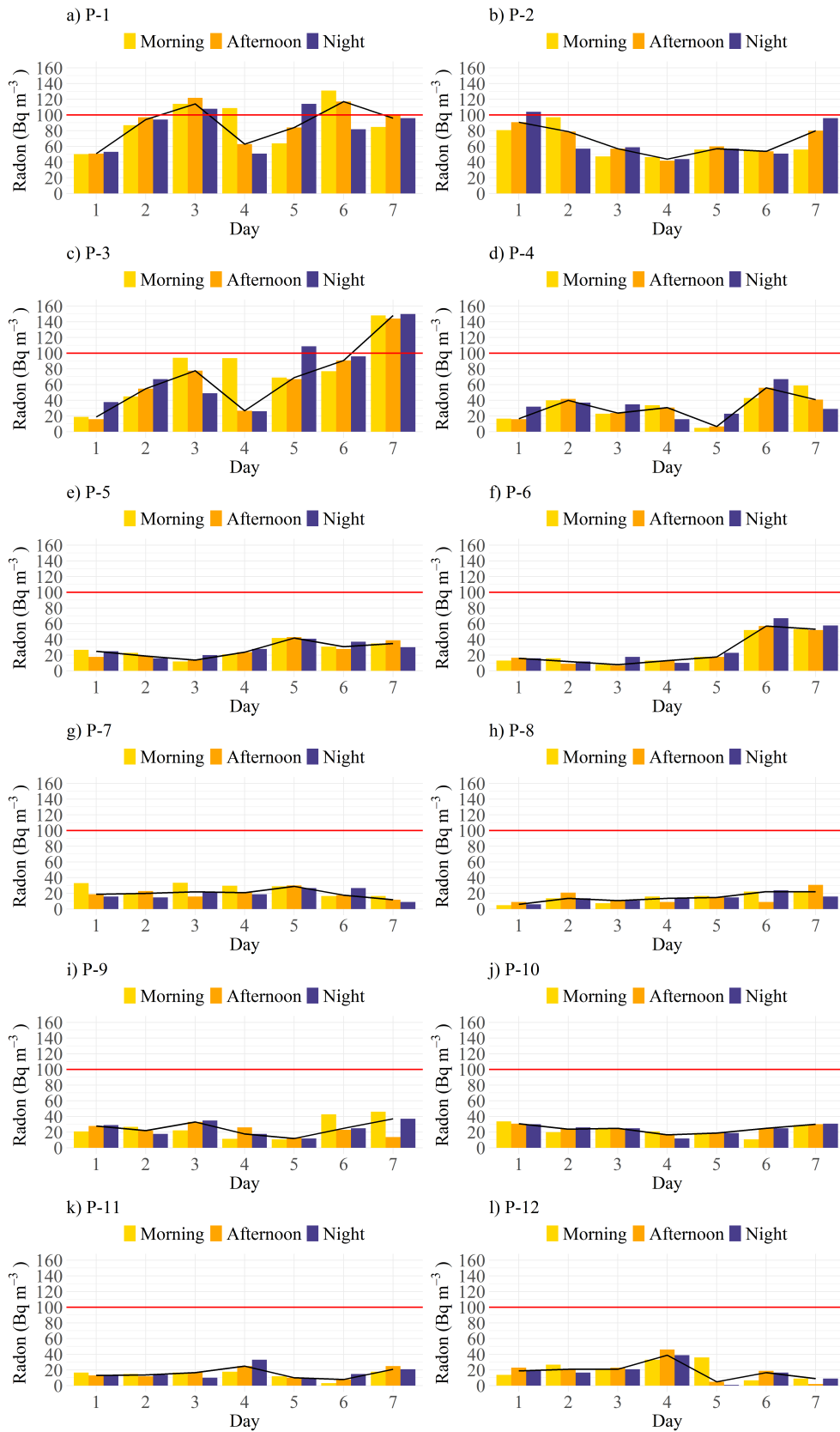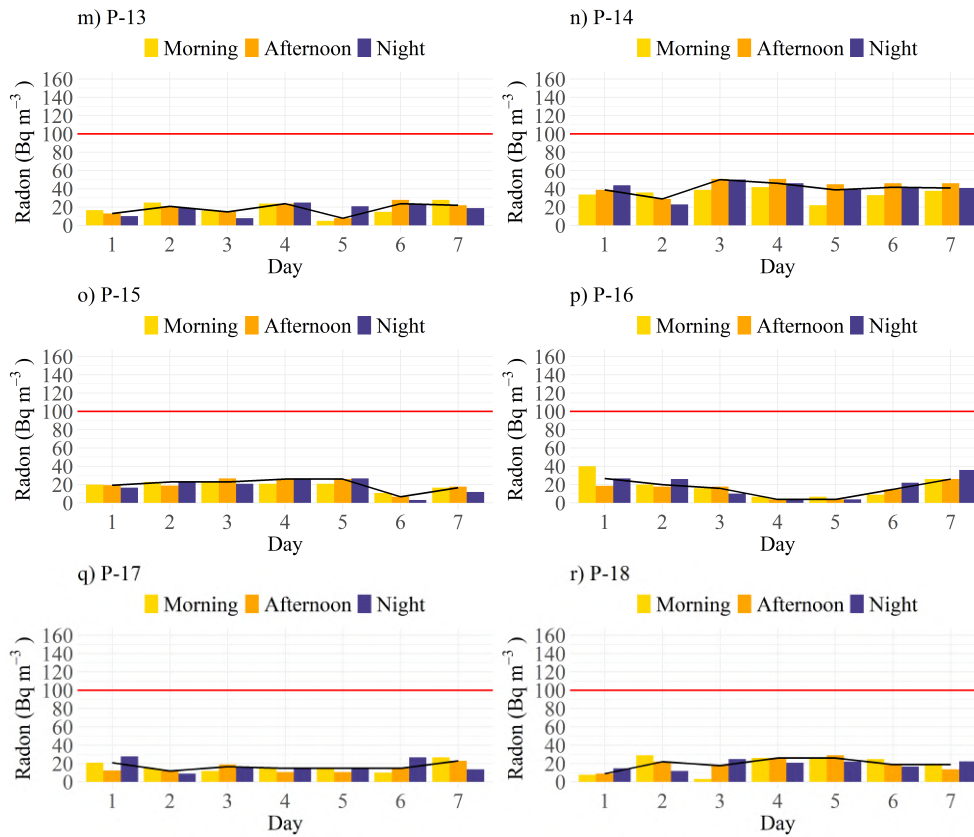
Figure 5.1: Daily average radon variability in Patrimonial houses. Daily radon measurements taken at morning (yellow), afternoon (orange), and night (blue) intervals over a 7-day period are depicted for each of the Patrimonial houses (a) to (r). The black line represents the median value of each day, with a horizontal red line indicating the WHO-recommended reference level of 100 $Bq\,m^{-3}$. Consistent height scaling enables visual comparison across the dataset.

Figure 5.1 illustrates the variation in radon levels throughout the day in Patrimonial houses. Noticeable fluctuations in radon concentration are evident in houses P-1, P-2, and P-3 (Figure 5.1: a), b), and c)), contrasted by more stable readings in houses P-4 to P-18 (Figure 5.1: d) to r)).

Among Patrimonial houses, P-1, P-2, and P-3 recorded radon concentrations occasionally exceeding 100 $Bq\,m^{-3}$, whereas the remaining houses maintained levels below the WHO-recommended reference level.

5.1.2 Multifamiliares Apartments

The plots illustrating short-term daily radon values for Multifamiliares apartments are displayed in Figure 5.2.

In contrast to Patrimonial houses, none of the daily radon measurements in Multi-familiares apartments exceeded the 100 Bq m^{-3} reference level. Additionally, there were no apparent abrupt changes in radon concentration throughout the 7-day measurement period. Moreover, visually, Multifamiliares apartments appear to have lower radon values compared to Patrimonial houses.
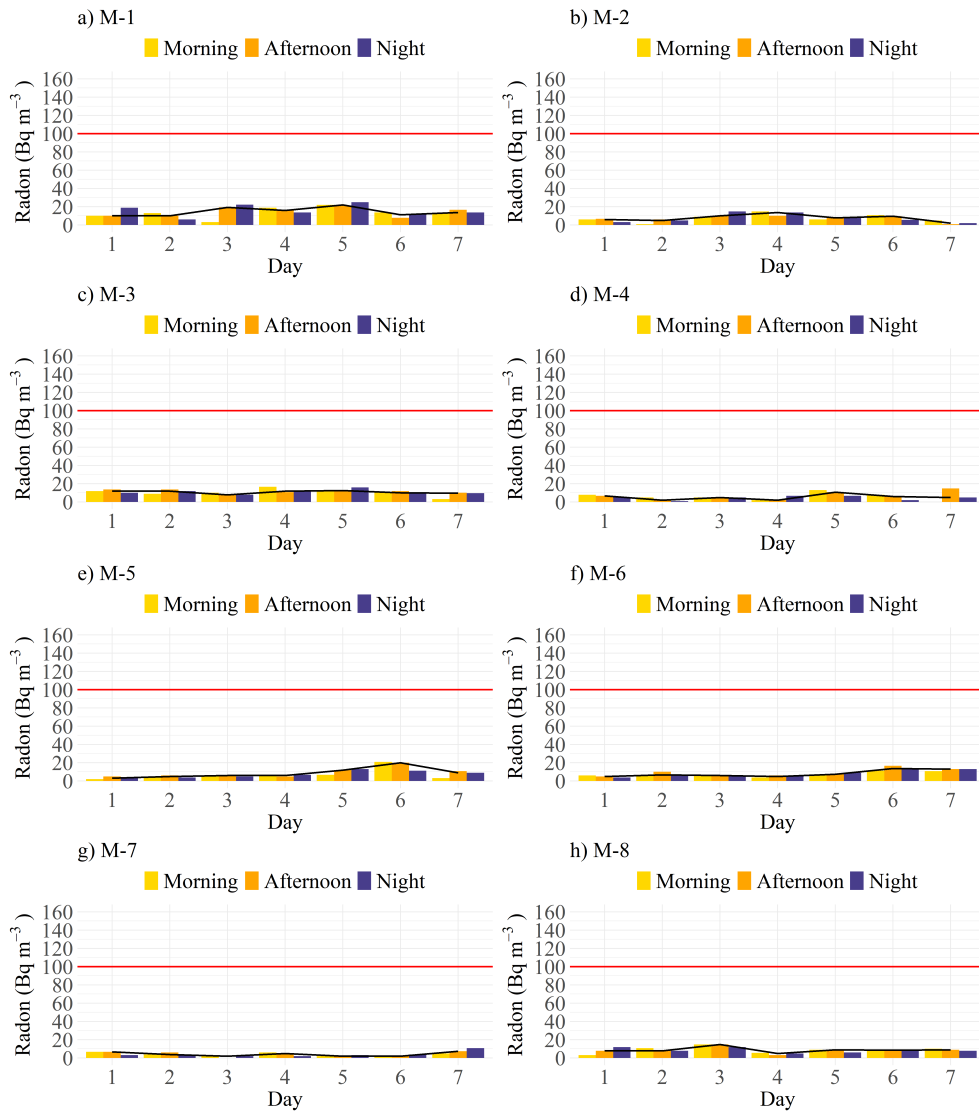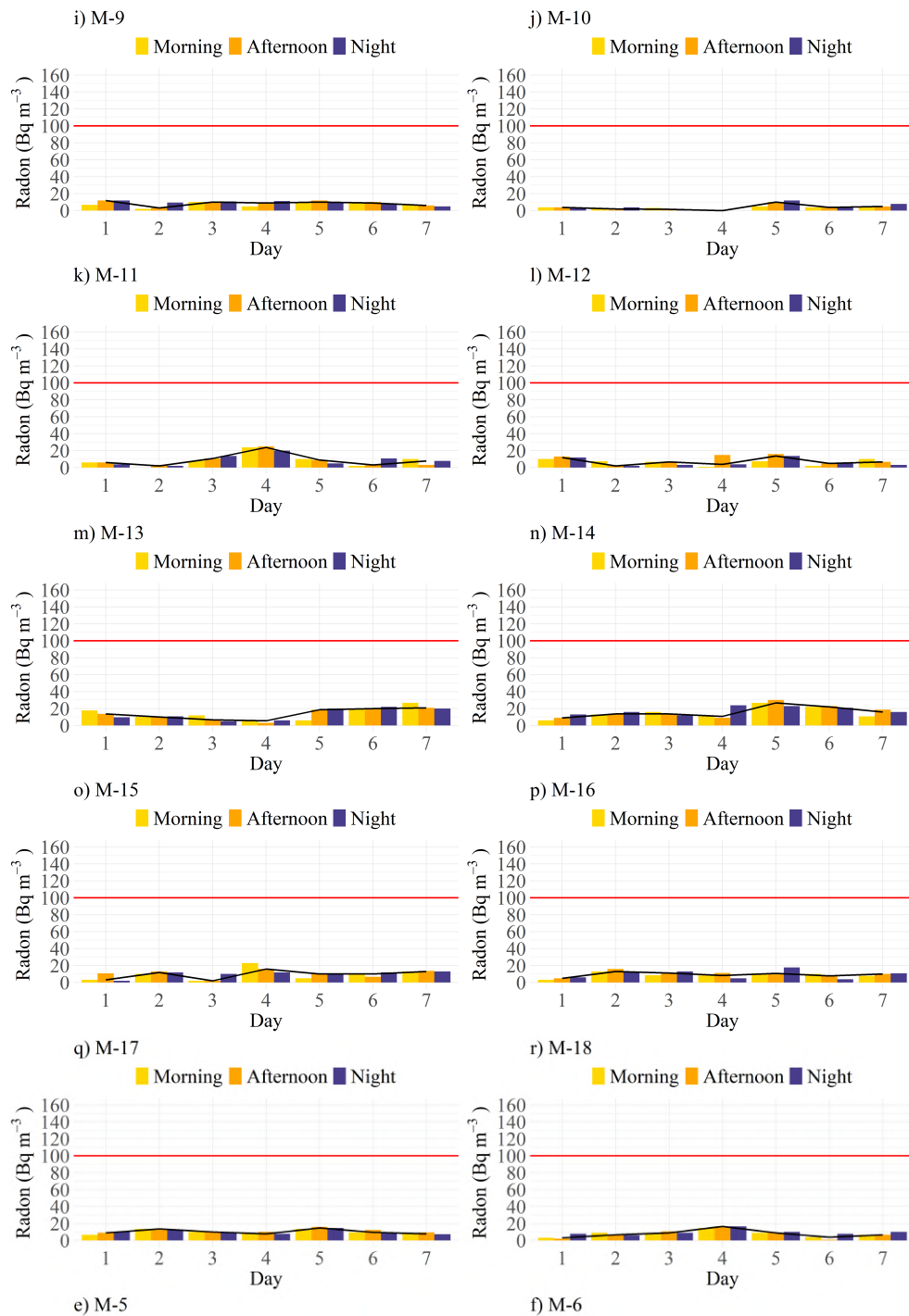
Figure 5.2: Daily average radon variability in Multifamiliares apartments. Daily radon measurements taken at morning (yellow), afternoon (orange), and night (blue) intervals over a 7-day period are depicted for each of the Multifamiliares apartments (a) to (r). The black line represents the median value of each day, with a horizontal red line indicating the WHO-recommended reference level of $100 \, \mathrm{Bq \, m^{-3}}$. Consistent height scaling enables visual comparison across the dataset.

5.2 Radon Relationship Between Relative Humidity and Temperature

5.2.1 Multidimensional Scaling

The results of the 7-day period of measuring three times per day (morning, afternoon, and night) of short-term 1-day radon concentration, inner temperature, inner-outer temperature difference, and relative humidity are uploaded in a GitHub repository [102]. To visualize the data a multidimensional scaling method was used. The method allows us to represent higher dimensional data into a, for example, 2-dimensional graph. In the Figure 5.3, it can be seen how the Multifamiliares apartments (triangle) and Patrimonial houses (circle) locate in the 2D graph. Colors represent the part of the day in which the measurements were taken, in yellow for morning, in orange for afternoon, and in purple for night.

Figure 5.3: Multidimensional scaling plot, showing the relationships between radon, temperature, and relative humidity. Patrimonial houses in circle, Multifamiliares apartments in triangle. Colors represent the part of the day in which the measurements were taken, in yellow for morning, in orange for afternoon, and in purple for night.

From Figure 5.3, the following observations can be made:

(i) Left part of the graph: In this part there are mainly Patrimonial houses in different

parts of the day.

(ii) Right upper part of the graph: In this region, there is a mix between Patrimonial houses and Multifamiliares apartments in different parts of the day.

(iii) Right lower part of the graph: Most of the houses in this region correspond to Multifamiliares apartments in different parts of the day.

5.2.2   Temperature

The study simultaneously tracked inner and outer temperatures alongside daily radon levels. Box plots were generated to aid in visually analyzing the data. Box plot of inner temperature by type of house and part of the day is presented in Figure 5.4.

Interestingly, Multifamiliares apartments exhibited notably higher inner temperatures compared to Patrimonial houses, as observed visually. This result may stem from the fact that during the measurement period, Patrimonial houses remained unoccupied.
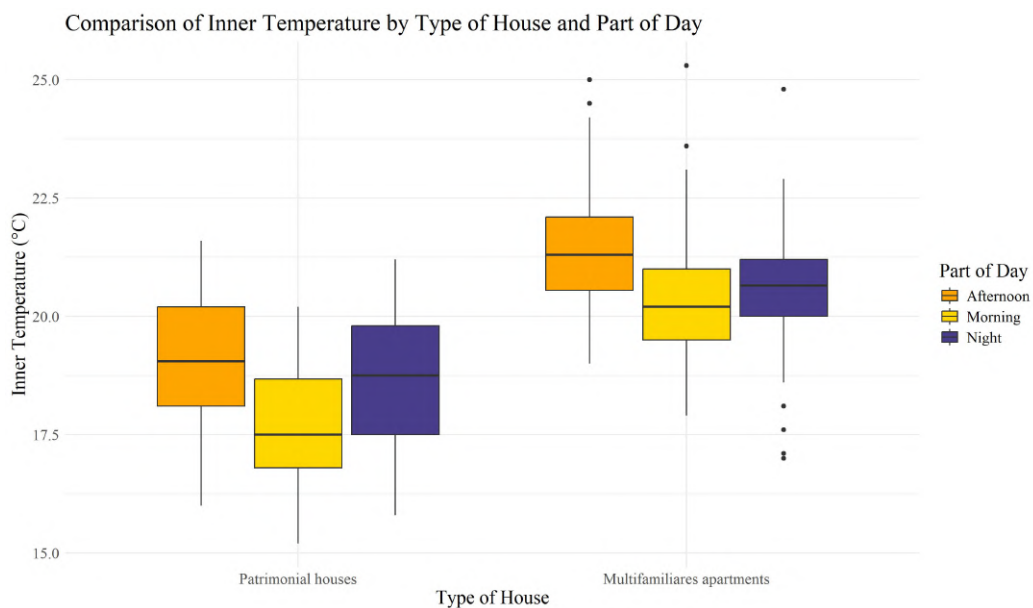
Figure 5.4: Box plot of inner temperature by type of house and part of the day. Morning (yellow), afternoon (orange), and purple (night).

Outer temperatures were also recorded. To better understand the influence of outer temperature, the difference between inner temperature and outer temperature was studied.

The box plot showing this difference by type of house and time of day is presented in Figure 5.5.
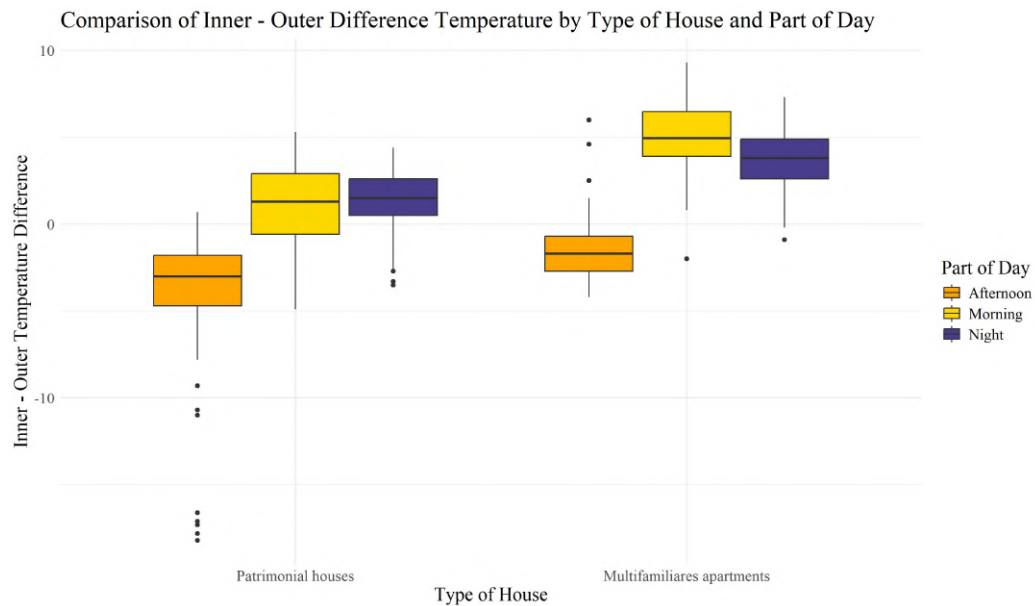
Figure 5.5: Box plot of the difference between inner and outer temperature by type of house and part of the day. Morning (yellow), afternoon (orange), and purple (night).

The difference between inner temperature and outer temperature is higher for Multifamiliares apartments as shown in Figure 5.5. These findings may be explained by the fact that Multifamiliares apartments are warmer than Patrimonial houses as shown in Figure 5.4.

5.2.3   Relative Humidity

Apart from oxygen, the air we inhale also includes moisture in the form of water vapor [103]. This moisture content plays a significant role in determining not only our comfort and health but also impacts the structural stability of our dwellings and possessions [103]. Humidity, denoting the quantity of water vapor present in the atmosphere, is crucial in this regard [103]. Expressed as Relative Humidity (RH), measured in percentage, it signifies the proportion of water vapor the air holds compared to its maximum capacity at a given temperature and pressure [103]. Temperature variations influence RH, thus leading to seasonal discrepancies [103]. Typically, residential environments exhibit lower RH levels during winter and higher levels during summer [103].

Low RH, commonly observed below 30% during winter, can exacerbate skin allergies, induce eye irritation, and heighten the risk of respiratory infections [103]. Furthermore, it may foster the survival of certain viruses and cause physical manifestations such as cracked skin and increased static electricity [103]. Conversely, elevated RH levels, surpassing 55%, often stem from inadequate ventilation or substantial indoor moisture sources [103].

Figure 5.6 displays box plots illustrating the relative humidity distribution for both Patrimonial houses and Multifamiliares.
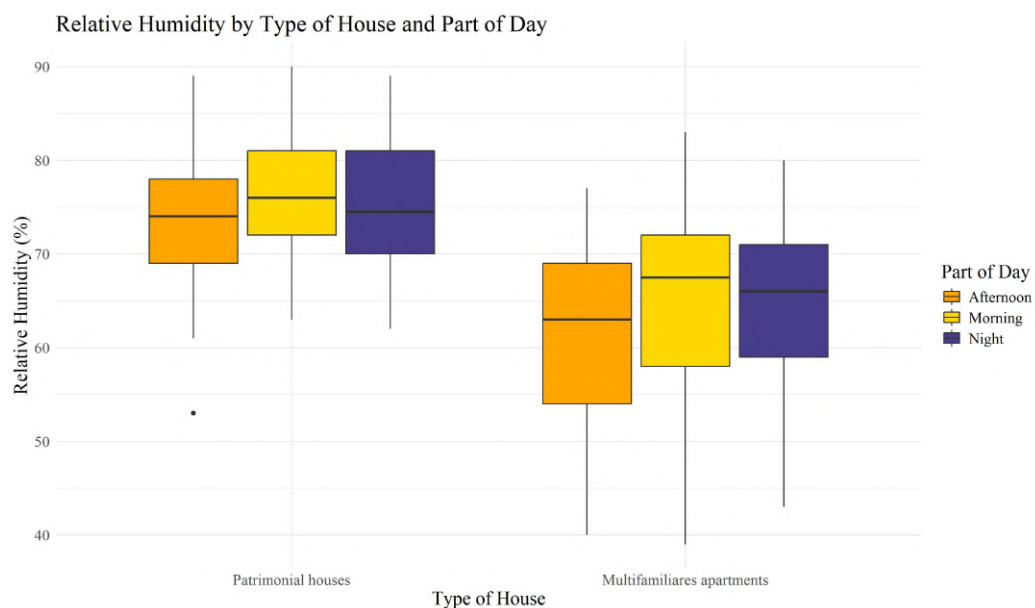
Figure 5.6: Box plot of relative humidity by type of house and part of the day. Morning (yellow), afternoon (orange), and purple (night).

Upon visual inspection, Patrimonial houses exhibit elevated relative humidity levels, typically ranging from 60% to 90%, whereas Multifamiliares apartments demonstrate a broader range, spanning from 35% to 85%. In fact, one of the primary reasons for the closure of Patrimonial houses pending further maintenance is the prevalence of humidity-related issues.

5.2.4   Correlations

Normality tests

Visually, the distributions of radon levels, inner-outer temperature, and relative humidity deviate from normality, as illustrated in Figures 5.7 and 5.8. Only inner temperature

appears to follow a normal distribution.

Notably, radon exhibits a right-skewed, approximately log-normal distribution. This is consistent with several studies that have shown similar shapes [83, 104, 105].
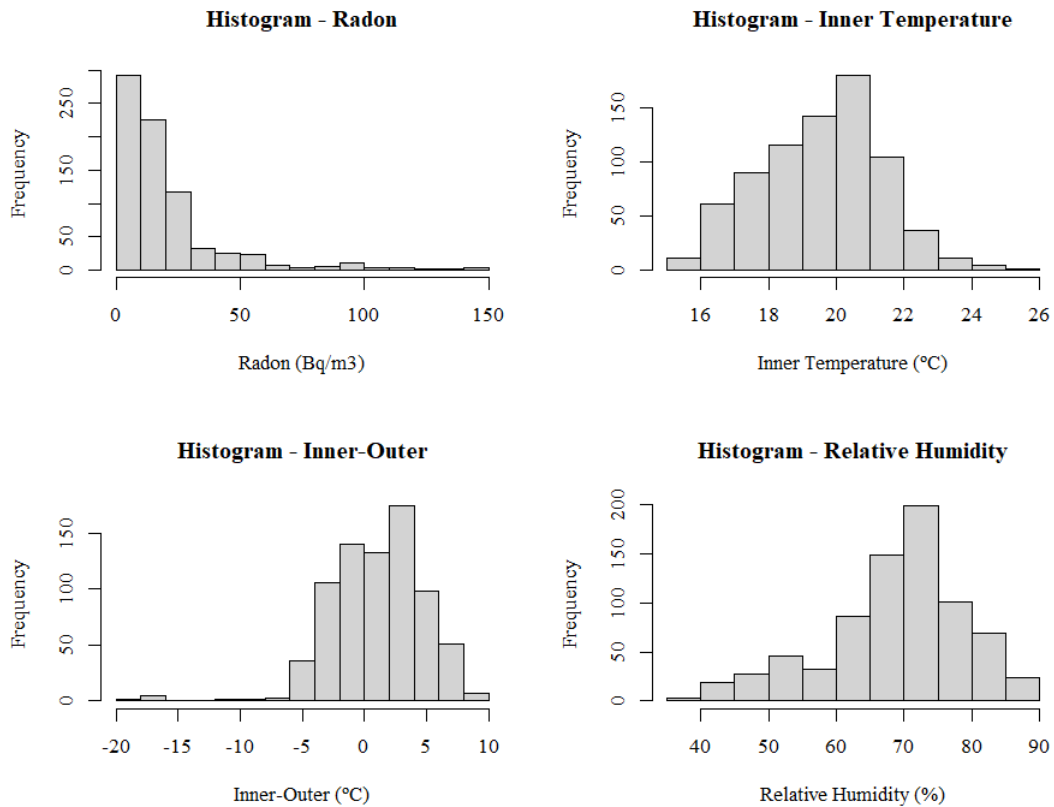
Figure 5.7: Visual representation of the histogram and density plot showcasing the distributions of radon levels, inner temperature, inner-outer temperature, and relative humidity.
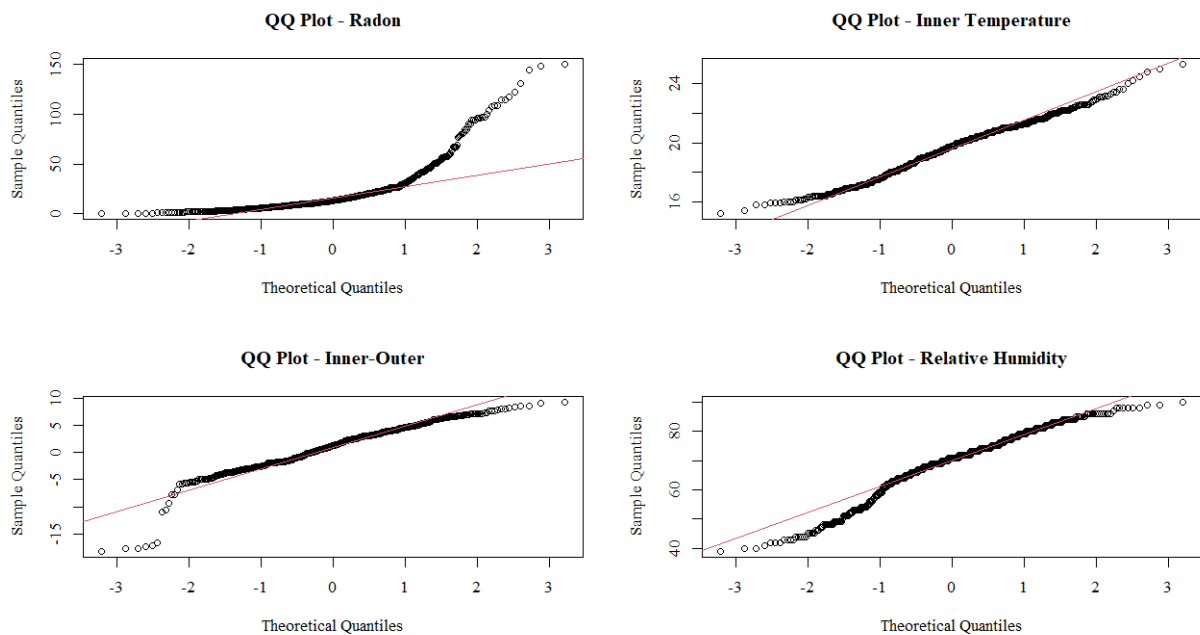
Figure 5.8: QQ plots of radon levels, inner temperature, inner-outer temperature, and relative humidity.

Kendall's rank correlation

Kendall's correlation test, also known as Kendall's rank correlation or Kendall's tau, is a statistical method used to measure the strength and direction of the relationship between two variables [106]. It is a non-parametric test, meaning it does not require the data to follow a specific distribution, such as normality, which is often an assumption in parametric tests [106].

Kendall's tau is calculated by comparing the ranking of two variables [106]. It counts the number of concordant pairs, where the ranks of both variables increase or decrease together, and the number of discordant pairs, where the ranks move in opposite directions [106]. The test statistic, tau, is then calculated as the difference between the number of concordant and discordant pairs, normalized by the total number of possible pairings [106].

The value of tau ranges from -1 (perfect negative correlation) to 1 (perfect positive correlation), with 0 indicating no correlation [106]. The closer the value is to 1 or -1, the stronger the correlation between the variables [106]. A positive tau indicates that as one variable increases, the other tends to increase as well, while a negative tau indicates that as one variable increases, the other tends to decrease [106].

The results of the Kendall's tau correlation test indicate the following:

(i) There is a low negative correlation between inner temperature and radon (p-value $<$ 2.2×10^{-16}, tau = -0.30).

(ii) There is a low negative correlation between indoor-outdoor temperature and radon concentration (p-value $< 2.2 \times 10^{-16}$, tau = -0.21).

(iii) There is a medium positive correlation between relative humidity and radon concentration (p-value $< 2.2 \times 10^{-16}$, tau = 0.33).

All three calculated correlations yielded statistically significant results. In this study, radon concentration demonstrated a negative correlation with indoor and outdoor temperatures, while exhibiting a positive correlation with relative humidity. It is important to note that the variability of radon levels depends on a multitude of factors, leading to potentially differing results in the literature. For instance, in a study by Xie et al. (2015), indoor radon concentrations were found to be negatively correlated with indoor humidity (correlation coefficient R = -0.14, p < 0.01) and outdoor temperature (correlation coefficient R = 0.3, p < 0.01), while positively correlated with the indoor-outdoor temperature difference (correlation coefficient R = 0.32, p < 0.05) [107].

In a separate investigation, radon concentration exhibited negative correlations with both indoor temperature (R = -0.22) and relative humidity (R = -0.31) [108]. Additionally, another study revealed a positive correlation between relative humidity and radon, supported by Spearman correlation analysis (rho = 0.12, p < 0.05), and a negative correlation with indoor temperature (rho = -0.53, p < 0.001) [109]. These findings are consistent with the outcomes observed in this research.

It is essential to acknowledge that temperature and relative humidity were recorded three times per day over a 7-day measurement period. However, this limited sampling frequency might not fully capture the diurnal variations in these parameters. Therefore, employing continuous monitoring of temperature and relative humidity, coupled with a continuous radon monitoring device, would offer a more comprehensive understanding of the intricate relationships among the variables under study.

5.3   Mean Radon Concentration and Annual Effective Dose

Mean radon concentration and annual mean effective dose values are presented in Table 5.1. Mean radon concentration corresponds to the 7-day value displayed by the Corentium Home radon detector. These values were used to calculate the annual effective dose using equation 4.1. Table 5.1 also shows additional information such as a code and time period. The code is a combination of a letter and a number, where 'P' denotes Patrimonial house, and 'M' represents Multifamiliares apartment. The numerical component of the code is determined based on the references provided in Figure 4.7. Notably, due to the utilization of three radon detectors, measurements were conducted during different time periods, allowing for a maximum of three houses to be studied concurrently. The column named as Time Period indicates which houses were examined simultaneously within the same time frame; starting from 0, for the first houses studied.

From Table 5.1, it can be seen that most of the houses have low levels of radon (< 100 Bq m^{-3}), which are below the reference level recommended by organizations such as the WHO and the ICRP. Due to low levels of radon, the annual effective dose is also low and within the recommended levels in most of the houses. P-1 and P-2 show higher values of radon and thus annual effective dose. At first, it could be thought that it could be due to an increase in environmental radon levels since these two houses are close to each other and were measured in the same time period. However, P-3 was also studied during the same time period and is next to P-2, but the radon levels found in P-2 are relatively low, so the differences could be attributed to other factors.

The minimum and maximum mean radon concentration values were found in M-6 and P-2, with 2.96 Bq m^{-3} and 130.95 Bq m^{-3}, respectively. The mean radon concentration is 20.58 Bq m^{-3}, the geometric mean is 13.99 Bq m^{-3}, and the median is 13.88 Bq m^{-3}.

To calculate the effective dose, 8,760 hours were used, which corresponds to the number of hours in a year. Considering that the average radon levels remained below the reference thresholds, it was expected that the calculated annual effective dose values would fall within acceptable limits. The ICRP recommends an annual effective dose from radon exposure to be maintained below 3-10 mSv y^{-1}, a criterion fulfilled by most of the houses [3]. Notably,

Table 5.1: Mean radon concentrations and annual effective doses.

Code	Radon (Bq m^{-3})	Annual Effective Dose (mSv y^{-1})	Time Period
P-1	94.72	2.39	5
P-2	130.98	3.30	5
P-3	18.87	0.48	5
P-4	33.67	0.85	4
P-5	29.97	0.76	4
P-6	32.93	0.83	4
P-7	21.83	0.55	1
P-8	12.95	0.33	1
P-9	24.79	0.63	1
P-10	24.79	0.63	2
P-11	16.65	0.42	2
P-12	19.98	0.50	0
P-13	17.76	0.45	2
P-14	41.81	1.05	0
P-15	19.98	0.50	3
P-16	14.8	0.37	3
P-17	16.65	0.42	3
P-18	19.98	0.50	0
M-1	12.95	0.33	10
M-2	7.77	0.20	6
M-3	7.77	0.20	9
M-4	4.81	0.12	11
M-5	7.77	0.20	10
M-6	2.96	0.07	9
M-7	3.7	0.09	12
M-8	7.77	0.20	7
M-9	9.99	0.25	8
M-10	3.7	0.09	12
M-11	7.77	0.20	12
M-12	5.92	0.15	11
M-13	11.84	0.30	9
M-14	16.65	0.42	11
M-15	9.99	0.25	8
M-16	10.73	0.27	7
M-17	7.77	0.20	6
M-18	7.77	0.20	10

among the Patrimonial houses, P-2 displayed the highest annual effective dose at 3.30 mSv y^{-1}.

Utilizing the mean radon concentrations outlined in Table 5.1, an indoor map illustrating radon concentration distributions for both Patrimonial houses and Multifamiliares apartments was generated and presented as Figure 5.9. The majority of the surveyed residences exhibited low radon levels, indicated by concentrations below 100 $Bq\,m^{-3}$, depicted in blue. One dwelling demonstrated moderate radon concentrations falling within the range of 70 - 100 $Bq\,m^{-3}$, while only a single residence exhibited elevated radon levels surpassing 100 $Bq\,m^{-3}$, represented by the color red.
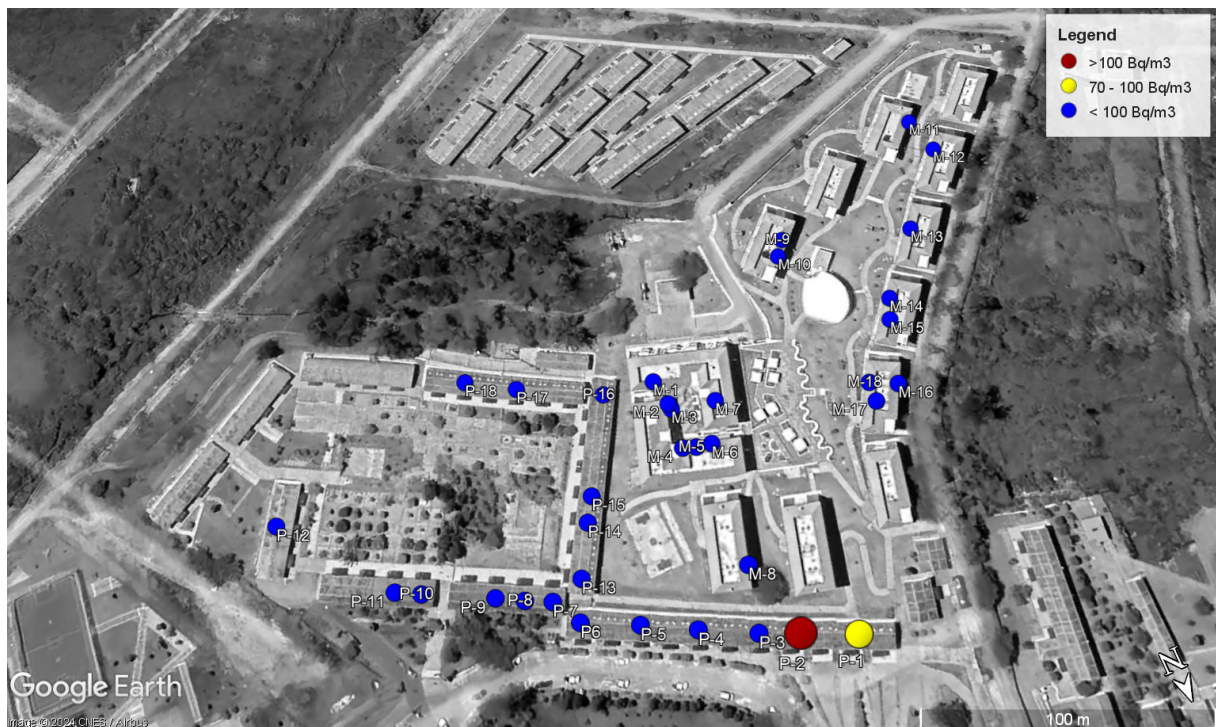
Figure 5.9: Radon concentration distributions for both Patrimonial houses and Multifamiliares. In blue values below 100 $Bq\,m^{-3}$, in yellow values between 70 - 100 $Bq\,m^{-3}$, and in red values surpassing 100 $Bq\,m^{-3}$.

5.4 Radon Concentration by Type of House

To visualize the radon levels by type of house, a bar plot was created. The y-axis represents the radon concentration, and the x-axis represents the house code. The graph shows the houses in increasing order from left to right, and a color is given to differentiate between

Patrimonial houses in red and Multifamiliares apartments in turquoise. Figure 5.10 displays the bar plot.
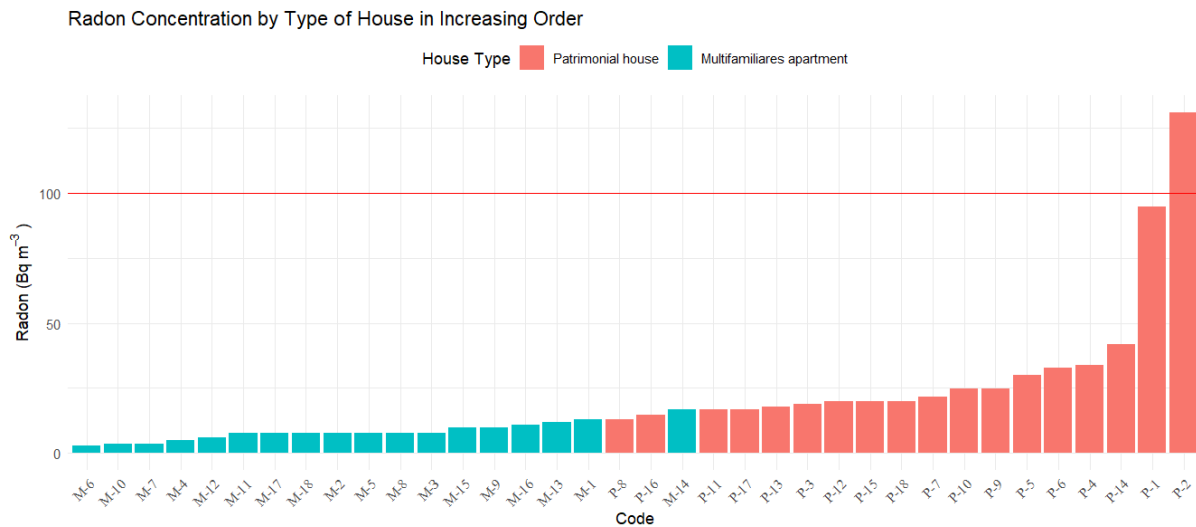
Figure 5.10: Bar plot of radon values by type of house organized in an increasing order from left to right. In red are Patrimonial houses and in turquoise Multifamiliares apartments. A red line is draw at 100 Bq m^{-3} which is the reference proposed by the WHO.

From Figure 5.10, it can be observed that most of the Patrimonial houses are located on the right side of the image, which corresponds to higher levels of radon. This visual observation suggests that there may be a difference in radon concentrations between Patrimonial houses and Multifamiliares apartments. To assess this finding, statistical analysis was used.

To assess the normality of the data, a Shapiro-Wilk Test was performed on both groups: Patrimonial houses and Multifamiliares apartments. The results showed the following:

(i) Multifamiliares apartments group: The distribution of radon concentration in this group follows a normal distribution, as indicated by a p-value of 0.25.

(ii) Patrimonial houses group: The distribution of radon concentration in this group does not follow a normal distribution, as indicated by a p-value of less than 0.05 (p-value $= 6.95 \times 10^{-6}$). Since the data in the Patrimonial houses group is not normally distributed, a non-parametric test should be used to compare the groups.

The Mann-Whitney U test is a suitable non-parametric test for comparing the distributions of two independent groups. It determines if there is a significant difference in the

central tendencies (medians) of a continuous variable (radon concentrations) between the groups, without assuming a normal distribution or equal variances. The results of the test showed a statistically significant difference (p-value $= 5.14 \times 10^{-7}$) in radon concentrations between Patrimonial houses and Multifamiliares apartments. In other words, the data supports the idea that the two groups have different median radon concentrations.

5.5 Limitations

5.5.1 Data Collection Limitation

One limitation in data collection was the restricted number of radon sensors, with only three available for the study. Increasing the number of detectors would have enhanced the sample size, enabling simultaneous radon measurements in all houses under study, thereby providing a more comprehensive dataset.

5.5.2 Impact of Unoccupied Patrimonial Houses

The unoccupied status of the Patrimonial houses during the study posed a limitation. Lack of human occupation affected ventilation, a crucial factor in radon level reduction. Moreover, inner temperature is affected by human activities, body heat, and cooking.

5.5.3 Data Logging Constraints

Temperature, relative humidity, and radon measurements were limited by the data logging capabilities, allowing only three readings per day over a 7-day period. This sparse data collection may not accurately capture the daily fluctuations of these variables, potentially obscuring valuable information.

5.5.4 Time Constraints

Time constraints also impacted the study, as a decision was made to reduce measuring time to include more houses. This choice excluded long-term measurements, which are essential for assessing actual long-term radon values. Although short-term 7-day averages

were similar to long-term values, the manufacturer recommends a minimum of 30 days of measurement for reliable long-term estimates.

By addressing these limitations in future studies, a more robust and comprehensive analysis of radon levels in Patrimonial houses can be achieved.

5.6   Comparison with Other Studies

Table 5.2 presents similar studies performed in Ecuador and other countries. The radon concentration in houses on Yachay Tech's campus ranges from 2.96 to 130.98 $\mathrm{Bq\,m^{-3}}$, with an average of 20.58 $\mathrm{Bq\,m^{-3}}$. Generally, the mean radon concentrations were below the reference level of 100 $\mathrm{Bq\,m^{-3}}$ established by the WHO. Moreover, the mean average radon concentration is significantly lower than the calculated Ecuadorian mean radon concentration of 94.30 $\mathrm{Bq\,m^{-3}}$ [110]. Recent studies conducted in Riobamba and Cuenca reported mean radon concentrations of 32 $\mathrm{Bq\,m^{-3}}$ and 35 $\mathrm{Bq\,m^{-3}}$, respectively [93, 94]. Thus, the radon concentration measured in San Miguel de Urcuquí is comparatively lower.

The methodology used in this study is similar to those employing a Corentium Home digital radon sensor. The devices were placed in living areas, such as bedrooms, where sunlight and moisture do not reach the device, following the manufacturer's recommendations. The device was positioned at least 150 cm from the nearest door, window, or air vent, and 50 cm above floor level. The measurement locations were selected to ensure the devices would not be disturbed during the measurement period.

It was common in studies using the Corentium Home radon sensor to measure radon over short periods, typically 7 days, with many recording both short-term and long-term values. However, long-term values were not utilized in this study. The manufacturer recommends a minimum of 30 days to obtain reliable long-term measurements, a consideration overlooked in some studies reporting long-term data.

Using the mean radon concentration obtained from the short-term 7-day measurements, a radon indoor map was created to visualize radon concentrations. Various methods can represent the data, such as interpolating and extrapolating to create a comprehensive color map showing radon distribution, as shown in Figure 3.11 [11]. In this study, radon concentrations were differentiated by color: houses with radon levels above 100 $\mathrm{Bq\,m^{-3}}$

were represented in red, those close to this value in yellow, and those with low values in blue. This color-coding is similar to the representation used in other studies, as shown in Figures 3.9 and 3.10.

Regarding correlations between radon and indoor temperature, indoor-outdoor temperature difference, and relative humidity, this study found that radon correlates negatively with temperature and indoor-outdoor temperature difference, while positively correlating with relative humidity. There is still some uncertainty regarding these relationships, as different studies report varying results. The variability of radon levels depends on multiple factors, leading to potentially differing results in the literature. For instance, a study by Xie et al. (2015) found indoor radon concentrations to be negatively correlated with indoor humidity (correlation coefficient R = -0.14, $p < 0.01$) and outdoor temperature (R = -0.30, $p < 0.01$), while positively correlated with the indoor-outdoor temperature difference (R = 0.32, $p < 0.05$) [107].

In another investigation, radon concentration showed negative correlations with both indoor temperature (R = -0.22) and relative humidity (R = -0.31) [108]. Additionally, another study revealed a positive correlation between relative humidity and radon, supported by Spearman correlation analysis (rho = 0.12, $p < 0.05$), and a negative correlation with indoor temperature (rho = -0.53, $p < 0.001$) [109]. These findings are consistent with the outcomes observed in this research. It is worth noting that, despite being statistically significant, the correlations between radon and both temperature and relative humidity were not strong.

Table 5.2: Comparison of radon levels found in this study with literature. Note: 'avg.' denotes average.

Location	Sample	Measuring Device	Measuring Time	Results (Bq m^{-3})	Reference
San Miguel de Urcuquí (Ecuador)	36	Corentium Home	7 days	2.96 - 130.98 (Avg. 20.58)	This study
Ecuador	61	Electrelet	Not specified	2.39 - 225.55 (Avg. 94.30)	[110]
Riobamba (Ecuador)	14	Corentium Home	7 days	2 – 95 (Avg. 32)	[93]
Cuenca (Ecuador)	47	Nuclear track detector with LR-115	90 days	8.33 - 148.33 (Avg. 35)	[94]
Kaya (Burkina Faso)	21	Corentium Home	7 days	2.89 - 197.11 (Avg. 28.47)	[78]
Ouagadougou (Burkina Faso)	21	Corentium Home	7 days	4.29 - 114.57 (Avg. 26.90)	[80]
Kirklareli (Turkey)	19	Corentium Home	7 days	16 - 77 (Avg. 40.8)	[81]
Koudougou (Burkina Faso)	24	Corentium Home	7 days	7.29 - 153.43	[79]
Qom (Iran)	123	Nuclear alpha track detector with CR-39	90 days	15 – 259	[15]
Madura Island (Indonesia)	95	Nuclear alpha track detector with CR-39	90 - 120 days	15.11 - 126.93 (Avg. 58.74)	[11]
Khorramabad (Iran)	56	Nuclear alpha track detector with CR-39	60 - 90 days	1.08 - 196.78 (Avg. 43.43)	[12]
Erzurum (Turkey)	110	Nuclear track detector with LR-115	60 days	11 - 380	[82]
Lima (Peru)	508	Nuclear track detector with LR-115	56 - 84 days	15 - 306 (Avg. 49)	[83]
Beijing (China)	800	Nuclear alpha track detector with CR-39	365 days	12.1 - 119.0 (Avg. 42.0)	[84]

Chapter 6

Conclusions and Recommendations

6.1   Conclusions

In the current investigation, a comprehensive assessment of indoor radon concentrations, temperature, and humidity was conducted across 36 residences in Yachay Tech Campus. The residences were categorized into two distinct groups: Patrimonial houses, representing older restored dwellings, and Multifamiliares apartments, embodying recently constructed homes. Each group comprised 18 residences, forming the basis of the analysis. The quantification of radon levels was facilitated through the utilization of the Corentium Home device by Airthings, which provided diverse readings. Specifically, the short-term 1-day average was recorded thrice daily over a span of 7 days, complemented by the determination of the short-term 7-day average at the conclusion of the 7-day interval. Simultaneous temperature and relative humidity measurements were taken using the HTC-1 device, synchronously with the radon 1-day average measurements. The 7-day assessment was adopted as the representative mean radon concentration.

The average radon concentration found in this study was 20.58 Bq m^{-3}, geometric mean 13.99 Bq m^{-3}, and median 13.88 Bq m^{-3}. Among the 36 residences investigated, residences P-1 and P-2 exhibited the most elevated levels of radon concentration, 94.72 Bq m^{-3} and 130.98 Bq m^{-3}, respectively. These values are notably higher in comparison to the remaining residences under study. Additionally, it is noteworthy that the radon concentration in P-2 surpassed the reference level of 100 Bq m^{-3} recommended by the WHO. Consequently,

long-term measurements and remedial actions should be considered. Conversely, residence M-6 displayed the lowest radon concentration at 2.96 Bq m^{-3}.

The short-term 7-day average radon values from different houses were used to create an indoor radon map of the Yachay Tech campus, contributing to the existing knowledge by providing localized data on indoor radon. Moreover, the radon concentrations in this zone were found to be lower than those reported in other parts of Ecuador. For instance, Riobamba and Cuenca reported mean radon concentrations of 32 Bq m^{-3} and 35 Bq m^{-3}, respectively. Thus, the radon concentration measured in San Miguel de Urcuquí is comparatively lower.

Given that the mean radon levels were below reference levels, it was anticipated that the calculated annual effective dose values would also fall within acceptable ranges. ICRP recommends an annual effective dose from radon exposure to remain below 3-10 mSv y^{-1}, a criterion met by the majority of the houses [3]. Among them, P-2 exhibited the highest annual effective dose at 3.30 mSv y^{-1} . It is crucial to acknowledge that this value is expected to decrease due to reduced occupancy during vacations and holidays.

A scrutiny of radon concentration distribution revealed that Patrimonial houses consistently exhibited elevated radon levels compared to the Multifamiliares apartments. This disparity was substantiated through statistical analysis, specifically the Mann-Whitney U test, which confirmed the significant differentiation between these groups. Hence, a clear distinction in radon levels emerges when juxtaposing the older-restored Patrimonial houses with the modern-built Multifamiliares apartments.

Notably, correlations were established between indoor temperature, the difference between indoor and outdoor temperatures, relative humidity, and radon concentration. A negative correlation between indoor temperature and radon levels was observed, implying an inverse relationship wherein radon levels rise as temperatures decrease. Similarly, as the indoor-outdoor temperature difference decreases or becomes negative, radon levels tend to increase. In contrast, a positive correlation was found between relative humidity and radon concentration, indicating that elevated humidity levels correspond to heightened radon concentrations.

It is noteworthy that Patrimonial houses exhibited elevated levels of radon concentration in comparison to Multifamiliares apartments. These differences corresponded with

lower indoor temperatures and narrower temperature differentials between indoor and outdoor environments in the Patrimonial houses. While the observed correlations between temperature and relative humidity in this study reached statistical significance, their strength was relatively modest. It suggests that additional factors beyond these variables may be influencing radon concentration levels.

Significantly, the Patrimonial houses remained unoccupied throughout the study period, potentially impacting indoor temperature and radon levels. Occupancy typically elevates indoor temperatures due to human activity, cooking, and other daily routines. Furthermore, radon concentrations often diminish with increased ventilation; thus, the act of opening windows and doors could effectively lower radon levels. Moreover, considerations such as architectural design, building materials, and structural integrity, including the presence of cracks in the foundations, may also contribute to variations in radon concentrations within the housing units.

6.2   Recommendations for Future Research

The first recommendation concerns the sample studied and the type of detectors used. In this study, 36 houses were monitored over a 7-day period using only three Corentium Home digital radon detectors, limited by sensor availability. This type of sensor may not be suitable for large-scale studies where radon is the main variable, due to its relatively high cost compared to other devices such as alpha track detectors.

The second recommendation involves the devices used to measure the correlated variables. In this study, radon short-term values were recorded three times per day over a 7-day period, along with indoor and outdoor temperatures and indoor relative humidity. Recording only three readings per day per house may not accurately reflect trends in temperature changes and relative humidity. The sensors used did not have data logging capabilities, so values were recorded manually by visiting each location. This issue could be resolved by using sensors with data logging functions. Specifically for radon, professional-grade radon detectors should be used to assess its relationship with other environmental variables. Although these detectors may be more expensive for large-scale studies, a balance should be considered.

Measuring radon concentrations is crucial for identifying this issue. Therefore, more radon surveys are encouraged, especially in countries like Ecuador, where there is no national regulation on this issue and the general population is largely unaware of it.

Bibliography

[1] World Health Organization, *WHO handbook on indoor radon: a public health perspective.* World Health Organization, 2009.

[2] ICRP, "Icrp publication 126: Radiological protection against radon exposure," *Annals of the ICRP*, vol. 43, pp. 5–73, 09 2014.

[3] International Comission on RadiologicalProtection (ICRP), "The 2007 recommendations of the international commission on radiological protection. icrp publication 103," *Ann ICRP*, vol. 37, no. 2.4, p. 2, 2007.

[4] A. Robertson, J. Allen, R. Laney, and A. Curnow, "The cellular and molecular carcinogenic effects of radon exposure: A review," *International Journal of Molecular Sciences*, vol. 14, no. 7, pp. 14 024–14 063, 2013. [Online]. Available: https://www.mdpi.com/1422-0067/14/7/14024

[5] Canadian Nuclear Safety Commission, "Radon and health," March 2011. [Online]. Available: https://api.cnsc-ccsn.gc.ca/dms/digital-medias/February-2011-Info-0813-Radon-and-Health-INFO-0813_e.pdf/object?subscription-key=3ff0910c6c54489abc34bc5b7d773be0

[6] C. Jia, Q. Wang, X. Yao, and J. Yang, "The role of dna damage induced by low/high dose ionizing radiation in cell carcinogenesis," *Exploratory Research and Hypothesis in Medicine*, vol. 6, no. 4, pp. 177–184, Dec 2021. [Online]. Available: https://www.xiahepublishing.com/2472-0712/ERHM-2021-00020

[7] G. Gillmore, R. Crockett, and T. Przylibski, ""igcp project 571: Radon, health and natural hazards" preface," *Natural Hazards and Earth System Sciences*, vol. 10, pp. 2051–2054, 10 2010.

[8] A. Grzywa-Celińska, A. Krusiński, J. Mazur, K. Szewczyk, and K. Kozak, "Radon—the element of risk. the impact of radon exposure on human health," *Toxics*, vol. 8, no. 4, 2020. [Online]. Available: https://www.mdpi.com/2305-6304/8/4/120

[9] A. Maier, J. Wiedemann, F. Rapp, F. Papenfuß, F. Rödel, S. Hehlgans, U. S. Gaipl, G. Kraft, C. Fournier, and B. Frey, "Radon exposure—therapeutic effect and cancer risk," *International Journal of Molecular Sciences*, vol. 22, no. 1, 2021. [Online]. Available: https://www.mdpi.com/1422-0067/22/1/316

[10] R. Bersimbaev, A. Pulliero, O. Bulgakova, A. Kussainova, A. Aripova, and A. Izzotti, "Radon biomonitoring and microrna in lung cancer," *International Journal of Molecular Sciences*, vol. 21, no. 6, 2020. [Online]. Available: https://www.mdpi.com/1422-0067/21/6/2154

[11] Wahyudi, I. D. Winarni, and M. Wiyono, "Indoor radon measurements in madura dwellings," *Journal of Physics: Conference Series*, vol. 1436, no. 1, p. 012012, jan 2020. [Online]. Available: https://dx.doi.org/10.1088/1742-6596/1436/1/012012

[12] H. Hassanvand, M. S. Hassanvand, M. Birjandi, b. kamarehie, and a. jafari, "Indoor radon measurement in dwellings of khorramabad city, iran," *Iranian Journal of Medical Physics*, vol. 15, no. 1, pp. 19–27, 2018. [Online]. Available: https://ijmp.mums.ac.ir/article_9552.html

[13] A. Maier, J. Jones, S. Sternkopf, E. Friedrich, C. Fournier, and G. Kraft, "Radon adsorption in charcoal," *International Journal of Environmental Research and Public Health*, vol. 18, no. 9, 2021. [Online]. Available: https://www.mdpi.com/1660-4601/18/9/4454

[14] C. Papastefanou, "Measuring radon in soil gas and groundwaters: A review," *Annals of Geophysics*, vol. 50, 08 2007.

[15] M. Fahiminia, R. Fouladi Fard, R. Ardani, A. Mohammadbeigi, K. Naddafi, and M. a. Hassanvand, "Indoor radon measurements in residential dwellings in qom, iran," *International Journal of Radiation Research*, vol. 14, no. 4, 2016. [Online]. Available: http://ijrr.com/article-1-1818-en.html

[16] Yachay Tech University, "History of the campus," https://www.yachaytech.edu.ec/en/about/history-of-the-campus/, (Accessed Aug. 08, 2023].

[17] L. T. N. Ngoc, D. Park, and Y.-C. Lee, "Human health impacts of residential radon exposure: Updated systematic review and meta-analysis of casendash;control studies," *International Journal of Environmental Research and Public Health*, vol. 20, no. 1, 2023. [Online]. Available: https://www.mdpi.com/1660-4601/20/1/97

[18] World Health Organization and others, *WHO guidelines for indoor air quality: selected pollutants.* World Health Organization. Regional Office for Europe, 2010.

[19] C. A, F. López, M. Arnaud, A. Oliveira, R. Neman, J. Hadler, P. Iunes, S. de Paulo, M. Osorio, R. Aparecido, R. C, M. V, V. R, G. Espinosa, J. Golzarri, T. Martinez, N. M, C. I, N. Segovia, and L. Sajó-Bohus, "Indoor radon measurements in six latin american countries," *Geofísica Internacional*, vol. 41, 10 2002.

[20] M. Donya, M. Radford, A. ElGuindy, D. Firmin, and M. H. Yacoub, "Radiation in medicine: Origins, risks and aspirations," *Global Cardiology Science and Practice*, vol. 2014, no. 4, 2015. [Online]. Available: https://www.qscience.com/content/journals/10.5339/gcsp.2014.57

[21] H. Omer, "Radiobiological effects and medical applications of non-ionizing radiation," *Saudi Journal of Biological Sciences*, vol. 28, no. 10, pp. 5585–5592, 2021. [Online]. Available: https://www.sciencedirect.com/science/article/pii/S1319562X21004502

[22] International Commission on Non-Ionizing Radiation Protection (ICNIRP), "Principles for non-ionizing radiation protection," *Health Physics*, vol. 118, no. 5, pp. 477–482, May 2020. [Online]. Available: https://doi.org/10.1097/hp.0000000000001252

[23] P. Sowa, J. Rutkowska-Talipska, U. Sulkowska, K. Rutkowski, and R. Rutkowski, "Ionizing and non-ionizing electromagnetic radiation in modern medicine," *Polish Annals of Medicine*, vol. 19, no. 2, pp. 134–138, 2012. [Online]. Available: https://www.sciencedirect.com/science/article/pii/S1230801312000380

[24] K. Hansson Mild, R. Lundström, and J. Wilén, "Non-ionizing radiation in swedish health care—exposure and safety aspects," *International Journal of Environmental Research and Public Health*, vol. 16, no. 7, 2019. [Online]. Available: https://www.mdpi.com/1660-4601/16/7/1186

[25] R. Clarke and T. R. Southwood, "Risks from ionizing radiation," *Nature (London);(United Kingdom)*, vol. 338, no. 6212, 1989.

[26] IARC Working Group on the Evaluation of Carcinogenic Risks to Humans and others, "Overall introduction," in *Ionizing Radiation, Part 1: X-and Gamma (γ)-Radiation, and Neutrons.* International Agency for Research on Cancer, 2000.

[27] B. Çalişkan and A. C. Çalişkan, "Interaction with matter of ionizing radiation and radiation damages (radicals)," in *Ionizing Radiation Effects and Applications*, B. Djezzar, Ed. Rijeka: IntechOpen, 2018, ch. 7. [Online]. Available: https://doi.org/10.5772/intechopen.74691

[28] C. Grupen, *Interaction of Ionizing Radiation with Matter.* Berlin, Heidelberg: Springer Berlin Heidelberg, 2010, pp. 31–56. [Online]. Available: https://doi.org/10.1007/978-3-642-02586-0_4

[29] P. Chaudhary, D. P. , D. Anca Oana, B. Yeskaliyeva, A. Razis, B. Modu, D. Calina, and J. Sharifi-Rad, "Oxidative stress, free radicals and antioxidants: potential crosstalk in the pathophysiology of human diseases," *Frontiers in Chemistry*, vol. 11, 05 2023.

[30] B. Q. Lee, T. Kibédi, A. E. Stuchbery, and K. A. Robertson, "Atomic radiations in the decay of medical radioisotopes: A physics perspective," *Computational and Mathematical Methods in Medicine*, vol. 2012, pp. 1–14, 2012. [Online]. Available: https://doi.org/10.1155/2012/651475

[31] C. Amsler, *Nuclear and Particle Physics*, ser. 2053-2563.   IOP Publishing, 2015. [Online]. Available: https://dx.doi.org/10.1088/978-0-7503-1140-3

[32] M. F. L'Annunziata, "Introduction: radioactivity and our well-being," in *Radioactivity.*   Elsevier, 2007, pp. 1–45.

[33] D. Jha, *Radioactivity and radioactive decay.*   Discovery Publishing House, 2004.

[34] S. Meschini, F. Laviano, F. Ledda, D. Pettinari, R. Testoni, D. Torsello, and B. Panella, "Review of commercial nuclear fusion projects," *Frontiers in Energy Research*, vol. 11, 06 2023.

[35] Q. Haider, "Nuclear fusion: Holy grail of energy," in *Nuclear Fusion*, I. Girka, Ed. Rijeka: IntechOpen, 2019, ch. 1. [Online]. Available: https://doi.org/10.5772/intechopen.82335

[36] M. Bonczyk, S. Chałupnik, N. Howaniec, A. Smoliński, and M. Wysocka, "Testing device for radon migration experiments, the construction and preliminary results," *Pure and Applied Geophysics*, vol. 176, no. 6, pp. 2557–2564, Jun 2019. [Online]. Available: https://doi.org/10.1007/s00024-019-02122-6

[37] Swiss Federal Office of Public Health, "Swiss radon handbook," 2000. [Online]. Available: https://www.bag.admin.ch/dam/bag/en/dokumente/str/srr/broschueren-radon/radon-technische-dokumentation-art-311-346.pdf.download.pdf/radon-technische-dokumentation-art-311-346.pdf

[38] *Modelling the Deposition of Airborne Radionuclides into the Urban Environment*, ser. TECDOC Series.   Vienna: INTERNATIONAL ATOMIC ENERGY AGENCY, 1994, no. 760. [Online]. Available: https://www.iaea.org/publications/5405/modelling-the-deposition-of-airborne-radionuclides-into-the-urban-environment

[39] L. Gulan, J. M. Stajic, D. Spasic, and S. Forkapic, "Radon levels and indoor air quality after application of thermal retrofit measures—a case study," *Air Quality, Atmosphere & Health*, vol. 16, no. 2, pp. 363–373, Feb 2023. [Online]. Available: https://doi.org/10.1007/s11869-022-01278-w

[40] ICRP, "Occupational intakes of radionuclides: part 3. icrp publication 137," *Ann. ICRP*, vol. 46, no. 3/4, pp. 1–486, 2017.

[41] N. R. Council *et al.*, "Health effects of exposure to low levels of ionizing radiation: Beir v," 1990.

[42] T. Tollefsen, G. Cinelli, P. Bossew, V. Gruber, and M. De Cort, "From the european indoor radon map towards an atlas of natural radiation," *Radiation protection dosimetry*, vol. 162, no. 1-2, pp. 129–134, 2014.

[43] W. Ellett, J. Fabrikant, and R. Cooper (INVITED), "BIER IV Committee Estimates of Lung Cancer Mortality Associated with Exposure to Radon Progeny," *Radiation Protection Dosimetry*, vol. 24, no. 1-4, pp. 445–449, 08 1988. [Online]. Available: https://doi.org/10.1093/oxfordjournals.rpd.a080321

[44] N. R. Council, *Health Effects of Exposure to Radon: BEIR VI.* Washington, DC: The National Academies Press, 1999. [Online]. Available: https://nap.nationalacademies.org/catalog/5499/health-effects-of-exposure-to-radon-beir-vi

[45] S. Darby, D. Hill, H. Deo, A. Auvinen, J. Barros-Dios, H. Baysson, F. Bochicchio, R. Falk, S. Farchi, A. Figueiras, M. Hakama, I. Heid, N. Hunter, L. Kreienbrock, M. Kreuzer, F. Lagarde, I. Mäkeläinen, C. Muirhead, W. Oberaigner, and R. Doll, "Residential radon and lung cancer - detailed results of a collaborative analysis of individual data on 7,148 persons with lung cancer and 14,208 persons without lung cancer from 13 epidemiological studies in europe." *Scandinavian journal of work, environment health*, vol. 32, pp. 1–83, 02 2006.

[46] D. Krewski, J. Lubin, J. Zielinski, M. Alavanja, V. Catalan, R. W. Field, J. Klotz, E. Létourneau, C. Lynch, J. Lyon, D. Sandler, J. Schoenberg, D. Steck, J. Stolwijk, C. Weinberg, and H. Wilcox, "A combined analysis of north american case-control studies of residential radon and lung cancer," *Journal of toxicology and environmental health. Part A*, vol. 69, pp. 533–97, 05 2006.

[47] J. H. Lubin, Z. Y. Wang, J. D. Boice Jr, Z. Y. Xu, W. J. Blot, L. De Wang, and R. A. Kleinerman, "Risk of lung cancer and residential radon in china: Pooled

results of two studies," *International Journal of Cancer*, vol. 109, no. 1, pp. 132–137, 2004. [Online]. Available: https://onlinelibrary.wiley.com/doi/abs/10.1002/ijc.11683

[48] F. Adrović, "Introductory chapter: Radon phenomenon," in *Radon*, F. Adrovic, Ed. Rijeka: IntechOpen, 2017, ch. 1. [Online]. Available: https://doi.org/10.5772/intechopen.70170

[49] D. Esan, M. Sridhar, R. Obed, Y. Ajiboye, B. Olubodun, and O. Oni, "Determination of residential soil gas radon risk indices over the lithological units of a southwestern nigeria university," *Scientific Reports*, vol. 10, 04 2020.

[50] J. Mazur and K. Kozak, "Complementary system for long term measurements of radon exhalation rate from soil," *Review of Scientific Instruments*, vol. 85, no. 2, 2014.

[51] N. Chau, E. Chruściel, and L. Prokólski, "Factor controlling measurement of radon mass exhalation rate," *Journal of environmental radioactivity*, vol. 82, pp. 363–9, 02 2005.

[52] G. Song, B. Zhang, X. Wang, J. Gong, D. Chan, J. Bernett, and S. Lee, "Indoor radon levels in selected hot spring hotels in guangdong, china," *Science of The Total Environment*, vol. 339, no. 1, pp. 63–70, 2005. [Online]. Available: https://www.sciencedirect.com/science/article/pii/S0048969704005856

[53] F. Ullah, S. Muhammad, and W. Ali, "Radon concentration and potential risks assessment through hot springs water consumption in the gilgit and chitral, northern pakistan," *Chemosphere*, vol. 287, 02 2022.

[54] United Nations Scientific Committee on the Effects of Atomic Radiation and Annex, B and others, "Exposures from natural radiation sources," *Cosmic rays*, vol. 9, no. 11, 2000.

[55] J.-W. Chung, T.-I. Hyon, and G.-S. Kim, "Effect of Temperature and Humidity on Indoor Radon Concentration," *International Journal of Trend in Scientific Research and Development*, vol. 4, no. 2, pp. 688–693, Feb. 2020. [Online]. Available: https://doi.org/10.5281/zenodo.3842955

[56] A. Sakoda, Y. Ishimori, and J. Tschiersch, "Evaluation of the intake of radon through skin from thermal water," *Journal of radiation research*, vol. 57, no. 4, pp. 336–342, 2016.

[57] M. Malakootian, Z. Khashi, F. Iranmanesh, and M. Rahimi, "Radon concentration in drinking water in villages nearby rafsanjan fault and evaluation the annual effective dose," *Journal of Radioanalytical and Nuclear Chemistry*, vol. 302, pp. 1167–1176, 2014.

[58] S. Keith, J. R. Doyle, C. Harper, M. Mumtaz, O. Tarrago, D. W. Wohlers, G. L. Diamond, M. Citra, and L. E. Barber, *Toxicological profile for radon.* Agency for Toxic Substances and Disease Registry (US), 2012.

[59] T. C. Carvalho, J. I. Peters, and R. O. Williams III, "Influence of particle size on regional lung deposition–what evidence is there?" *International journal of pharmaceutics*, vol. 406, no. 1-2, pp. 1–10, 2011.

[60] A. Sakoda, Y. Ishimori, A. Kawabe, T. Kataoka, K. Hanamoto, and K. Yamaoka, "Physiologically based pharmacokinetic modeling of inhaled radon to calculate absorbed doses in mice, rats, and humans," *Journal of nuclear science and technology*, vol. 47, no. 8, pp. 731–738, 2010.

[61] W. Hofmann, "Modelling inhaled particle deposition in the human lung—a review," *Journal of Aerosol Science*, vol. 42, no. 10, pp. 693–724, 2011.

[62] G. M. Kendall and T. J. Smith, "Doses to organs and tissues from radon and its decay products," *Journal of Radiological Protection*, vol. 22, no. 4, p. 389, dec 2002. [Online]. Available: https://dx.doi.org/10.1088/0952-4746/22/4/304

[63] A. Khursheed, "Doses to systemic tissues from radon gas," *Radiation Protection Dosimetry*, vol. 88, 2000.

[64] A. Sakoda, Y. Ishimori, K. Fukao, K. Yamaoka, T. Kataoka, and F. Mitsunobu, "Lung dosimetry of inhaled radon progeny in mice," *Radiation and environmental biophysics*, vol. 51, pp. 425–442, 2012.

[65] A. Sakoda, Y. Ishimori, K. Yamaoka, T. Kataoka, and F. Mitsunobu, "Absorbed doses of lungs from radon retained in airway lumens of mice and rats," *Radiation and environmental biophysics*, vol. 52, pp. 389–395, 2013.

[66] National Research Council, *Risk Assessment of Radon in Drinking Water.* National Academies Press, Jun. 1999. [Online]. Available: https://doi.org/10.17226/6287

[67] M. M. Ouellette, S. Zhou, and Y. Yan, "Cell signaling pathways that promote radioresistance of cancer cells," *Diagnostics*, vol. 12, no. 3, 2022. [Online]. Available: https://www.mdpi.com/2075-4418/12/3/656

[68] J. Nickoloff, L. Taylor, N. Sharma, and T. Kato, "Exploiting dna repair pathways for tumor sensitization, mitigation of resistance, and normal tissue protection in radiotherapy," *Cancer Drug Resistance*, vol. 4, 06 2021.

[69] R.-X. Huang and P.-K. Zhou, "Dna damage response signaling pathways and targets for radiotherapy sensitization in cancer," *Signal Transduction and Targeted Therapy*, vol. 5, no. 1, May 2020. [Online]. Available: https://doi.org/10.1038/s41392-020-0150-x

[70] E. I. Azzam, J.-P. Jay-Gerin, and D. Pain, "Ionizing radiation-induced metabolic oxidative stress and prolonged cell injury," *Cancer Letters*, vol. 327, no. 1, pp. 48–60, 2012, special Issue: Oxidative Stress-Based Cancer Biomarkers. [Online]. Available: https://www.sciencedirect.com/science/article/pii/S0304383511007592

[71] J. Sia, R. Szmyd, E. Hau, and H. E. Gee, "Molecular mechanisms of radiation-induced cancer cell death: A primer," *Frontiers in Cell and Developmental Biology*, vol. 8, 2020. [Online]. Available: https://www.frontiersin.org/articles/10.3389/fcell.2020.00041

[72] X. Dang, H. Lin, Y. Li, X. Guo, Y. Yuan, R. Zhang, X. Li, D. Chai, and Y. Zuo, "MicroRNA profiling in BEAS-2B cells exposed to alpha radiation reveals potential biomarkers for malignant cellular transformation," *Toxicology Research*, vol. 9, no. 6, pp. 834–844, 12 2020. [Online]. Available: https://doi.org/10.1093/toxres/tfaa094

[73] Z. Chen, D. Wang, C. Gu, X. Liu, W. Pei, J. Li, Y. Cao, Y. Jiao, J. Tong, and J. Nie, "Down-regulation of let-7 microrna increased k-ras expression in lung damage induced by radon," *Environmental Toxicology and Pharmacology*, vol. 40, no. 2, pp. 541–548, 2015. [Online]. Available: https://www.sciencedirect.com/science/article/pii/S1382668915300533

[74] Health Canada, "Guide for radon measurements in residential dwellings (Homes)," Government of Canada, June 2017, Canada.ca. [Online]. Available: https://www.canada.ca/en/health-canada/services/publications/health-risks-safety/guide-radon-measurements-residential-dwellings.html

[75] N. G. Barros, D. J. Steck, and R. W. Field, "A comparison of winter short-term and annual average radon measurements in basements of a radon-prone region and evaluation of further radon testing indicators," *Health Physics*, vol. 106, no. 5, pp. 535–544, May 2014. [Online]. Available: https://doi.org/10.1097/hp.0000000000000004

[76] T. Martinez, M. Navarrete, L. Cabrera, P. González, and A. Ramirez, "Relationship between short and long term radon measurements," *Radiation Physics and Chemistry*, vol. 61, no. 3, pp. 687–688, 2001, 8th International Symposium on Radiation Physics - ISRP8. [Online]. Available: https://www.sciencedirect.com/science/article/pii/S0969806X01003747

[77] Environmental Protection Agency, "What is EPA's action level for radon and what does it mean?" 2023, [Accessed 25-08-2023]. [Online]. Available: https://www.epa.gov/radon/what-epas-action-level-radon-and-what-does-it-mean

[78] W.-Y. Elola, L. Bambara, A. Doumounia, N. Kohio, S. Ouedraogo, and F. Zougmoré, "Assessment of radon concentrations inside residential buildings and estimation of the dose in the city of kaya, burkina faso," *Open Journal of Applied Sciences*, vol. 13, pp. 1066–1078, 01 2023.

[79] M. Derra, L. T. Bambara, K. Kaboré, Y. Z. Sawadogo, O. Cissé, and F. Zougmoré, "Measurement of Radon Concentration and Estimation of Cancer Risk in Twenty-

Four Model Houses in the Town of Koudougou," *Open Journal of Applied Sciences*, vol. 14, no. 1, pp. 193–204, Jan. 2024.

[80] B. T. Luc, K. Karim, D. Moumouni, B. Cedric, O. I. Cisse, and F. Zougmore, "Assessment of indoor radon concentration in residential buildings at ouagadougou and estimation of the annual effective dose," *Radiation Science and Technology*, vol. 7, no. 2, pp. 41–46, 2021. [Online]. Available: https://doi.org/10.11648/j.rst.20210702.14

[81] S. Özden and S. Aközcan Pehlivanoğlu, "Indoor radon levels in dwellings of kirklareli, turkey," *Sakarya University Journal of Science*, vol. 26, 02 2022.

[82] R. Durak, D. Kiran, E. Kavaz, and N. Ekinci, "Indoor radon measurements in erzurum province of turkey," *Journal of Physics: Conference Series*, vol. 707, no. 1, p. 012029, apr 2016. [Online]. Available: https://dx.doi.org/10.1088/1742-6596/707/1/012029

[83] P. Pereyra, C. J. Guevara-Pillaca, R. Liza, B. Pérez, J. Rojas, L. Vilcapoma L., S. Gonzales, L. Sajo-Bohus, M. E. López-Herrera, and D. Palacios Fernández, "Estimation of indoor 222rn concentration in lima, peru using lr-115 nuclear track detectors exposed in different modes," *Atmosphere*, vol. 14, no. 6, 2023. [Online]. Available: https://www.mdpi.com/2073-4433/14/6/952

[84] H. Wang, L. Zhang, P. Gao, and Q. Guo, "A pilot survey on indoor radon concentration in beijing," *Radiation Medicine and Protection*, vol. 3, no. 1, pp. 22–25, 2022. [Online]. Available: https://www.sciencedirect.com/science/article/pii/S266655572200003X

[85] S. M. Khan and S. Chreim, "Residents' perceptions of radon health risks: a qualitative study," *BMC Public Health*, vol. 19, no. 1, Aug. 2019. [Online]. Available: https://doi.org/10.1186/s12889-019-7449-y

[86] S. Rahman, M. Faheem, S. Rehman, and Matiullah, "Radon awareness survey in pakistan," *Radiation protection dosimetry*, vol. 121, no. 3, pp. 333–336, 2006.

[87] Y. Wang, C. Ju, A. D. Stark, and N. Teresi, "Radon awareness, testing, and reme-
diation survey among new york state residents," *Health Physics*, vol. 78, no. 6, pp.
641–647, 2000.

[88] N. Vogeltanz-Holm and G. G. Schwartz, "Radon and lung cancer: What does the
public really know?" *Journal of environmental radioactivity*, vol. 192, pp. 26–31,
2018.

[89] D. T. Esan, R. I. Obed, O. T. Afolabi, M. K. Sridhar, B. B. Olubodun, and
C. Ramos, "Radon risk perception and barriers for residential radon testing in
southwestern nigeria," *Public Health in Practice*, vol. 1, p. 100036, 2020. [Online].
Available: https://www.sciencedirect.com/science/article/pii/S2666535220300355

[90] F. A. García Paz, Y. A. Gonzalez Romero, and R. Zalakeviciute, "Radon (222Rn)
concentrations in the touristic Jumandy cave in the Amazon region of Ecuador,"
Journal of Radiation Research, vol. 60, no. 6, pp. 759–767, 10 2019. [Online].
Available: https://doi.org/10.1093/jrr/rrz064

[91] J. Orbe, J. L. Herrera-Robalino, G. Ureña-Callay, J. Telenchano-Ilbay, S. Samaniego-
León, A. Fienco-Bacusoy, A. Cando-Veintimilla, and T. Toulkeridis, "An evaluation
of radon in drinking water supplies in major cities of the province of chimborazo,
central andes of ecuador," *Water*, vol. 15, no. 12, 2023. [Online]. Available:
https://www.mdpi.com/2073-4441/15/12/2255

[92] J. Amancha, "Evaluación de la concentración del gas radón en ladrillos artesanales
en las parroquias: Juan montalvo-san sebastián e ignacio flores comunidad la vi-
centina de la ciudad latacunga, provincia de cotopaxi," B.S thesis, Ingeniería civil
y mecánica, Ingeniería civil, Universidad Técnica de Ambato, 2021, available at
https://repositorio.uta.edu.ec/jspui/handle/123456789/32363.

[93] J. Carrasco and C. Cuadrado, "Medición de la concentración de 222rn en residencias
y lugares de trabajo en la ciudad de riobamba," 09 2016.

[94] M. Loayza, "Elaboración de un mapa radiológico de los niveles de radón presentes
en las viviendas de las parroquias urbanas de la ciudad de cuenca - ecuador en

el periodo 2017 - 2018," B.S thesis, Ingeniería Ambiental, Universidad Politécnica Salesiana, 2018, available at http://dspace.ups.edu.ec/handle/123456789/15421.

[95] B. Castillo, "Cálculo del riesgo radiológico debido a la concentración de radón en los centros de educación inicial de la zona urbana y rural de cuenca, ecuador," B.S thesis, Ingeniería Ambiental, Universidad Politécnica Salesiana, 2016, available at http://dspace.ups.edu.ec/handle/123456789/12997.

[96] Yachay Tech University, "On-campus housing," https://www.yachaytech.edu.ec/en/vida-campus/residencias/, (Accessed Aug. 08, 2023].

[97] L. Ballance, "Radon: how is radon measured? how does an airthings device measure radon?" https://help.airthings.com/en/articles/3119759-radon-how-is-radon-measured-how-does-an-airthings-device-measure-radon, (Accessed Aug. 08, 2023].

[98] Airthings, "How we make the corentium home radon detector," https://www.airthings.com/resources/radon-detector, 2016, (Accessed Aug. 08, 2023].

[99] L. Ballance, "Corentium home: what do my measurements mean?" https://help.airthings.com/en/articles/3668763-corentium-home-what-do-my-measurements-mean, (Accessed Aug. 08, 2023].

[100] M. Yarahmadi, A. Shahsavani, M. H. Mahmoudian, N. Shamsedini, N. Rastkari, and M. Kermani, "Estimation of the residential radon levels and the annual effective dose in dwellings of shiraz, iran, in 2015," *Electronic physician*, vol. 8, no. 6, pp. 2497–2505, Jun. 2016. [Online]. Available: https://doi.org/10.19082/2497

[101] K. Hadad and J. Mokhtari, "Indoor radon variations in central iran and its geostatistical map," *Atmospheric Environment*, vol. 102, pp. 220–227, Feb. 2015. [Online]. Available: https://doi.org/10.1016/j.atmosenv.2014.12.013

[102] Jorge-Gutierrez-Guimi, "Jorge-gutierrez-guimi/datathesis: Start," Aug. 2023. [Online]. Available: https://doi.org/10.5281/zenodo.8305196

[103] Health Canada, "Relative humidity indoors: Factsheet," 2016. [Online]. Available: https://publications.gc.ca/collections/collection_2018/sc-hc/H144-33-2016-eng.pdf

[104] I. M. H. Angelika Schaffrath Rosario, Jürgen Wellmann and H.-E. Wichmann, "Radon epidemiology: Continuous and categorical trend estimators when the exposure distribution is skewed and outliers may be present," *Journal of Toxicology and Environmental Health, Part A*, vol. 69, no. 7-8, pp. 681–700, 2006. [Online]. Available: https://doi.org/10.1080/15287390500261190

[105] O. Alber, C. Laubichler, S. Baumann, V. Gruber, S. Kuchling, and C. Schleicher, "Modeling and predicting mean indoor radon concentrations in austria by generalized additive mixed models," *Stochastic Environmental Research and Risk Assessment*, vol. 37, no. 9, pp. 3435–3449, Sep 2023. [Online]. Available: https://doi.org/10.1007/s00477-023-02457-6

[106] *Kendall Rank Correlation Coefficient*. New York, NY: Springer New York, 2008, pp. 278–281. [Online]. Available: https://doi.org/10.1007/978-0-387-32833-1_211

[107] D. Xie, M. Liao, and K. Kearfott, "Influence of environmental factors on indoor radon concentration levels in the basement and ground floor of a building - a case study," *Radiation Measurements*, vol. 82, 08 2015.

[108] Z. Lounis-Mokrani, M. Allab, and M. Ziane, "Preliminary study of effect of environmental parameter variations on indoor radon concentrations in mediterranean climate," *International Journal of Low Radiation*, vol. 11, p. 115, 01 2019.

[109] G.-S. K. Jai-Won Chung, Tae-In Hyon, "Effect of temperature and humidity on indoor radon concentration," *International Journal of Trend in Scientific Research and Development (IJTSRD)*, vol. 4, no. 2, pp. 688–693, February 2020. [Online]. Available: https://www.ijtsrd.com/papers/ijtsrd30128.pdf

[110] A. Canoba, F. López, M. Arnaud, A. Oliveira, R. Neman, J. Hadler, P. Iunes, S. Paulo, A. Osorio, R. Aparecido, C. Rodrıguez, V. Moreno, R. Vasquez, G. Espinosa, J. Golzarri, T. Martınez, M. Navarrete, I. Cabrera, N. Segovia, P. Peña, E. Taméz, P. Pereyra, M. López-Herrera, and L. Sajo-Bohus, "Indoor

radon measurements and methodologies in latin american countries," *Radiation Measurements*, vol. 34, no. 1, pp. 483–486, 2001, proceedings of the 20th International Conference on Nuclear Track s in Solids. [Online]. Available: https://www.sciencedirect.com/science/article/pii/S1350448701002116
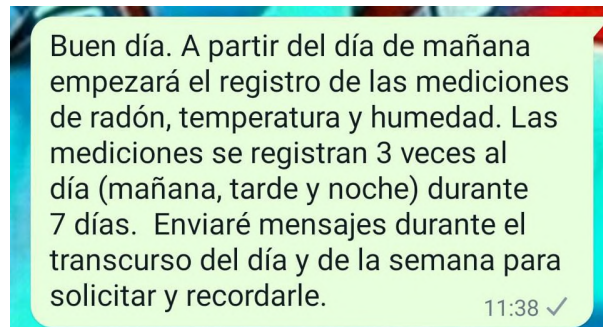
Appendices

.1   Appendix 1.

Figure 1: Conversation showing how the data was obtained when the sensors where placed in occupied houses.